



**Neurochirurgischen Klinik des Klinikums rechts der Isar der
Technischen Universität München**

Direktor: Univ.-Prof. Dr. Bernhard Meyer

The Analysis of Language-Related Tracts Based on nTMS Mapping in Patients with Left-Hemispheric Perisylvian Tumors

Haosu Zhang

Vollständiger Abdruck der von der Fakultät für Medizin der Technischen
Universität München zur Erlangung des akademischen Grades eines

Doktors der Medizin

genehmigten Dissertation.

Vorsitzende: Prof. Dr. Gabriele Multhoff

Prüfende/-r der Dissertation:

1. apl. Prof. Dr. Sandro M. Krieg
2. Priv. -Doz. Dr. Jens Gempt

Die Dissertation wurde am 12.01.2021 bei der Technischen Universität
München eingereicht und durch die Fakultät für Medizin am 08.06.2021
angenommen.

**für
meine Eltern**

Danksagung

Zunächst möchte ich mich meinen Doktorvater, Prof. Dr. med. Sandro Krieg für die Möglichkeit, meinen Doktor in seiner Arbeitsgruppe am Klinikum rechts der Isar durchführen zu können, herzlich bedanken. Durch seine kontinuierliche Hilfe und Unterstützung erweiterte ich nicht nur mein Fachwissen, sondern konnte auch wertvolle Einstellungen und Erfahrungen für eine praktische medizinische Karriere erlangen. Für uns Ärzte ist es besonders wichtig, neben dem praktischen Handwerk auch wissenschaftlich und präzise zu arbeiten und unsere praktische Arbeit auf aktuellen wissenschaftlichen Erkenntnissen zu stützen. Ich kann mir keinen besseren Betreuer, als Sie vorstellen!

Ich möchte auch meinen Mentor PD Dr. Dr. med. Nico Sollmann danken. Mit seiner Hilfe konnte ich mich hier im Labor und im Forschungsumfeld der TUM schnell eingewöhnen. Er unterstützte mich und meine Forschung tatkräftig und stand mir immer mit wertvollen Hinweisen und Tipps für mein Forschungsprojekt zur Seite.

Außerdem möchte ich Herrn Axel Schröder von Herzen danken, insbesondere für seine praktischen und technischen Hilfestellungen, sowohl mit der verwendeten Software als auch im Umgang mit dem nTMS-Gerät.

Ich möchte meinen Eltern (Shu-yi Cao und Wei-ming Zhang) und meine Familie danken, die mich ermutigen und mein Auslandsstudium unterstützen. Dank ihnen kann ich meinen Traum verwirklichen. Ich vermisse meine Oma und meinen Opa.

Am Ende möchte ich Ann-Katrin Ohlerth meinen Dank aussprechen, für ihre Geduld und wertvollen Anmerkungen beim Korrekturlesen meiner Dissertation, ganz besonders fürs Verbessern meiner Grammatikfehler. Gleichzeitig möchte ich mich bei Leonie Kram, Beate Neu, and Enrike Rosenkranz für ihre bedeutende Unterstützung bei der Übersetzung ins Deutsche bedanken. Vielen Dank auch an meine Freunde Severin, Lioba, Anna, Franziska und Marc. Sie machen mein Leben abwechslungsreich.

Während der COVID-19-Pandemie in Deutschland initiierte die Regierung das Rückführungsprogramm über das Außenministerium, um 200.000 deutsche Staatsbürger und ihre Familien zurückzubringen, die vorübergehend in Gebieten gestrandet sind, die besonders von Reisebeschränkungen betroffen sind. Es fördert mein Verständnis des richtigen Sozialmanagements.

TABLE OF CONTENTS

1.	ABBREVIATION.....	4
2.	INTRODUCTION.....	5
2.1	LANGUAGE PRESERVATION IN BRAIN TUMOR RESECTION	5
2.2	TRANSCRANIAL MAGNETIC STIMULATION	6
2.2.1	Background and development	6
2.2.2	Basic approach	8
2.2.3	Line- versus electric-field navigated TMS	8
2.2.4	nTMS and individualized localization of language function.....	9
2.2.5	nTMS-based DTI-FT for language function	10
2.3	LANGUAGE-RELATED FIBER TRACTS AND THEIR FUNCTIONS	11
2.3.1	Language-related neural tracts	11
2.3.2	Language-related dorsal and ventral streams	12
2.4	AIM OF THE CURRENT STUDY.....	13
3.	MATERIALS AND METHODS	15
3.1	ETHICS	15
3.2	PATIENTS AND STUDY INCLUSION.....	15
3.3	STUDY DESIGN AND CLINICAL EXAMINATION	15
3.4	MAGNETIC RESONANCE IMAGING	17
3.5	LANGUAGE MAPPING BY NTMS.....	18
3.5.1	Registration	18
3.5.2	Rough mapping.....	18
3.5.3	Angulation	19
3.5.4	Resting motor threshold determination	20
3.5.5	Cortical parcellation system template	21
3.5.6	Language mapping process.....	22
3.7	NTMS-BASED DTI-FT	26
3.8	STATISTICS.....	29
4.	RESULTS	31
4.1	CLINICAL AND DEMOGRAPHIC DATA.....	31
4.2	MAPPING AND TRACTOGRAPHY	35
4.3	RATIOS OF PATIENTS PRESENTING VISUALIZED FIBERS	38
4.4	NUMBERS OF FIBERS AND $RATIO_{FIBERS-PER-TRACT}$ IN TRACTOGRAPHY	38
4.5	ANALYSIS OF VENTRAL AND DORSAL STREAMS	39
5.	DISCUSSION.....	41
5.1	NTMS AND THE PROGNOSIS OF LANGUAGE FUNCTION	41
5.2	NTMS-BASED DTI-FT FOR LANGUAGE FUNCTION	42
5.3	LANGUAGE-RELATED TRACTS	43
5.4	DIFFERENT CATEGORIES OF NAMING ERRORS.....	45
5.5	VENTRAL/DORSAL STREAM & NTMS-BASED LANGUAGE-RELATED TRACTOGRAPHY	47
5.6	ADJUSTMENTS OF PARAMETERS IN DTI-FT	48
5.7	LIMITATION	49
6.	SUMMARY.....	51
6.1	ENGLISH.....	51
6.2	DEUTSCH.....	53
7.	REFERENCES.....	55

1. ABBREVIATION

3D: Three-Dimensional

ADM: Abductor Digiti Minimi

AF: Arcuate Fascicle

APB: Abductor Pollicis Brevis

ArF: Arcuate Fibers

BMRC: British Medical Research Council

BOLD-fMRI: Blood Oxygen Dependent Functional Magnetic Resonance Imaging

CF: Commissural Fibers

CNT: Corticonuclear Tract

CtF: Corticothalamic Fibers

DES: Direct Electrical Stimulation

DICOM: Digital Imaging and Communications in Medicine (DICOM)

DTI: Diffusion Tensor Imaging

EEG: Electroencephalography

En-TMS: E-field navigated TMS

FCR: Flexor Carpi Radialis

FLAIR: Fluid-attenuated Inversion Recovery

FoF: Fronto-occipital Fascicle

FT: Fiber Tracking

GTR: Gross Total Resection

HD: High Definition

ILF: Inferior Longitudinal Fascicle

IONM: Intraoperative Neuromonitoring

Ln-TMS: Line navigation TMS

MEG: Magnetoencephalography

MEP: Motor Evoked Potential

nTMS: Navigated Transcranial Magnetic Stimulation

PACS: Picture Archiving and Communication System

PET: Positron Emission Tomography

SLF: Superior Longitudinal Fascicle

UF: Uncinate Fascicle

2. INTRODUCTION

2.1 Language Preservation in Brain Tumor Resection

Cerebral tumors are commonly seen diseases in the neurosurgery department. More than half of them are characterized by malignant histopathological proliferation and gravely endangers human health (Adamson *et al.*, 2010). Resection is one of the major treatments when facing malignant neoplasms. Recently, it has been widely recognized that the balance between the Gross Total Resection (GTR) and the protection of normal cerebral functions should be carefully balanced to avoid severe restrictions in quality of life (Young *et al.*, 2015; Ogunlade *et al.*, 2019). Although an optimal extent of resection implementing the GTR is considered to be related to prolonged survival (Quinones-Hinojosa *et al.*, 2009; Matsuda *et al.*, 2018), the accompanying injuries may also bring about unavoidable functional deficits, especially when the tumor invades functionally eloquent cortical areas or important subcortical tracts related to functions, such as motor, sensation, language, or memory (Ahmadipour *et al.*, 2019). Therefore, it is realized among neurosurgeons that protecting patients' brain function during surgery – alongside achieving GTR – is of tremendous relevance (Duffau and Mandonnet, 2013).

Tumors occurring in eloquent cortical brain regions bearing specific functions account for 33.30% to 58.60% of intracranial tumors (Schreckenberger *et al.*, 2001; Tai and Piccini, 2004). The uncertainty, complexity, and individuality of the functional distribution in the brain have far exceeded the classic anatomical theory. Specifically, the modern models of verbal processing are based on the inter- and intra-network interaction, composed of parallel and interconnected streams involving both cortical and subcortical structures (Chang *et al.*, 2015). Analysis of individual functional distribution before surgery by neuroimaging and brain mapping technology can reduce the incidence of surgical-related complications or functional impairments (Calautti *et al.*, 2001; Kekhia *et al.*, 2011; Ottenhausen *et al.*, 2015).

Understanding of brain function has been further developed from the perspective of anatomical analysis to the dynamic relationship between brain function and structure (Ewert *et al.*, 2018). Recently, the development of neuroimaging and brain mapping has promoted individualized brain function testing and clinical applications (Ripolles *et al.*, 2016; Gordon *et al.*, 2017). Thus, the classical concept of brain function being localized only cortically within specific Brodmann areas seems more and more outdated.

In recent years, the studies on neural plasticity have gained extensive attention, suggesting the dynamic anatomic location of brain function, which is a good complement to the traditional concepts (Saito *et al.*, 2014; Xu *et al.*, 2017). Therefore, there is increasing evidence for reallocation of brain function on the cortical and subcortical level in patients with brain diseases, which forms the concept of plasticity. Specifically, the brain's responses to intracranial lesions involve the process of adaption and reconstruction following damage (Frost *et al.*, 2003). The necessary time, the changing degree, and the extent of the plasticity are all beyond the interpretation of classical functional anatomy. If these functional brain areas can be identified individually during perioperative stages, they could be protected during surgical procedures (Schulz *et al.*, 2012; Sharma *et al.*, 2013).

The protection of language function is a particular concern in modern neuro-oncological surgery. The language function is the tool in exchanging and passing information among human beings. Previous studies have demonstrated that the incidence of aphasia after resecting tumors located in language-eloquent regions ranged from 17% to 100% (Peraud *et al.*, 2004; Duffau *et al.*, 2008; Mayer, 2008; Lubrano *et al.*, 2010). With the development of neuroimaging and mapping technology, several methods for delineating language functions are accessible in most neurosurgery departments, aiming to investigate cerebral function during surgical preparation. Techniques include blood oxygen-dependent functional magnetic resonance imaging (BOLD-fMRI), diffusion tensor imaging (DTI), magnetoencephalography (MEG), positron emission tomography (PET), and electroencephalography (EEG). However, until now, the most important way to identify cerebral functions in a functional mapping approach is direct electrical stimulation (DES), which is usually considered as the gold standard for localizing cerebral function due to its direct measurement on the brain during operation (Borchers *et al.*, 2011; Muller *et al.*, 2018). It is worth noting that fMRI, DTI, and MEG as non-invasive neuroimaging methods can provide relevant functional information before surgery to improve the efficiency of DES mapping and facilitate the GTR during surgery (Ottenhausen *et al.*, 2015; Morrison *et al.*, 2016). With these techniques, functional mappings have become more credible, objectively presenting the distribution of functional brain areas and related subcortical functional anatomy. These functional mapping results can assist neurosurgeons in designing the surgical procedure accurately and are essential in decreasing the risk of surgery-related functional deficits.

Over the last decade, a non-invasive method, navigated transcranial magnetic stimulation (nTMS), has become a vital tool in identifying cerebral function preoperatively, which is in good consistency with intraoperative DES (Krieg *et al.*, 2013; Picht *et al.*, 2013). Specifically, nTMS can generate a virtual lesion through an induced electric field (e-field), thereby modulating related brain functions. At present, nTMS is commonly applied to analyze and localize cerebral regions of motor function and language function preoperatively in neurosurgical practice (Krieg *et al.*, 2015; Krieg *et al.*, 2017).

2.2 Transcranial Magnetic Stimulation

2.2.1 Background and development

TMS is a non-invasive technique to interfere with cerebral functions. The mechanism of TMS is that the capacitor currents discharge in the stimulation coil generating a magnetic field on the targeted regions, which then induces changes in the electrical field. When the changes are strong enough to depolarise the nerve cell membrane potential, their electrophysiological responses can be induced.

In 1985, Anthony Barker introduced TMS as a technique that permitted non-invasive stimulation of the cerebral cortex to explore its potential neurophysiological effects (Barker *et al.*, 1985). Since then, people have employed TMS to regulate and also detect cerebral functions. In the following years, the safety and therapeutic effects of TMS were demonstrated, which provided support for its clinical application (Bridgers, 1991). In 1997, the therapeutic effects of TMS were investigated on depression (Markwort *et al.*, 1997), and later on bipolar and unipolar disorders

(Nahas *et al.*, 1999).

In the last decade, neuro-navigation technologies have been developed rapidly in many neurosurgery centers. The most important progress has been made by tackling two issues. First, individualized, high-resolution three-dimensional (3D) reconstruction of the brain structural images was constructed based on the structural image. Second, the navigation system realizes the real-time visualization and recognition of anatomical structures in operating regions. This, meanwhile, provided a new solution for accurate targeting of stimuli: the optically tracked stereotactic neuro-navigation equipment and TMS coil were successfully combined for the precise localization of stimulation output. When all these factors were connected to a monitor system, it can generate real-time spatial and temporal information of the e-field on a re-constructed 3D brain from structural MRI scans on a screen, which together is called navigated transcranial magnetic stimulation (nTMS) (Krieg, 2017).

Previous studies found nTMS accurate and effective in mapping cortical motor and linguistic regions compared with DES (Picht *et al.*, 2013; Lehtinen *et al.*, 2018). The stimulation output intensity can be adjusted according to individual levels. Its inhibitory stimulus directly interferes with the processing of language tasks by the cerebral cortex, making it a unique advantage in identifying the language cortex. As demonstrated in multiple studies, the current spatial resolution of nTMS is in the range of 5 – 10 mm (Brasil-Neto *et al.*, 1992; Ravazzani *et al.*, 1996; Thielscher and Kammer, 2002; Toschi *et al.*, 2008; Sliwinska *et al.*, 2014). nTMS-based motor mapping has a high concordance with intraoperative DES (Krieg *et al.*, 2012b; Sollmann *et al.*, 2015d) and, likewise, was better in preoperative function localization than fMRI and MEG (Picht *et al.*, 2013; Tarapore *et al.*, 2013; Krieg *et al.*, 2017). Specifically, among the above-mentioned other functional imaging and mapping techniques, the sensitivity and specificity of nTMS-based motor mapping are superior to others compared with DES (Jack *et al.*, 1994; Lehericy *et al.*, 2000; Tomczak *et al.*, 2000; Picht *et al.*, 2013). In the interpretation of the results of the functional mapping, no sophisticated post-processing algorithms are needed in nTMS analysis compared with fMRI or MEG (Suri *et al.*, 2002; Tewarie *et al.*, 2014). The spatial resolution of nTMS can provide accurate brain structure location and corresponding functional information for surgery. DES, as an invasive procedure, is routinely used during surgery for localizing function eloquent regions. The standard DES was an electrified electrode placed directly on the cortical or subcortical tissues to identify the cerebral functions after craniotomy. When combined with electromyography (EMG), it can analyze the motor function, or combined with language tests during intraoperative awake procedures, language-related brain regions can be localized (Riva *et al.*, 2016; Southwell *et al.*, 2016). However, it is worth noting that not every patient can cooperate to perform the language test during the intraoperative awake period. In previous work, it demonstrated that 4.2% failed awake craniotomy is caused by lack of intraoperative communication with the patient, and 2.1% caused by intraoperative seizures (Nossek *et al.*, 2013a; Nossek *et al.*, 2013b). DES measurements were not available for detecting their function for these patients; therefore, the substitute tests are in need. In these cases, the preoperative functional mapping technique is a good supplement to DES for identifying relevant brain tissues in order to protect brain function. Furthermore, the add-on value of preoperative functional neuroimaging and mapping is demonstrated in the case of suggesting the potential eloquent regions during DES mapping (Picht *et al.*, 2013). Currently, the most widely used perioperative functional imaging techniques were fMRI, MEG, and nTMS. To

guarantee their effectiveness and safety, it was necessary to identify their accuracy, precision, availability, economic effectiveness, and so on. Some published studies compared these techniques with intraoperative DES as the gold-standard method, and they will be further described in the following parts.

2.2.2 Basic approach

Navigated TMS can be utilized as a potential strategy, on the one hand, for treating psychosocial diseases and nerve rehabilitation (Lioumis *et al.*, 2012a; Julkunen *et al.*, 2016) and the other hand, identifying function-related cerebral regions through precisely navigated stimulation (Krieg *et al.*, 2012b; Krieg *et al.*, 2014a). The latest navigation system is currently based on e-field monitoring and is more accurate in localization than conventional line navigation (Sollmann *et al.*, 2016a).

TMS generates a strong and quickly changing magnetic field by inducing a short capacitor discharge of electric current via a coil against the scalp (Terao and Ugawa, 2002; Peng *et al.*, 2018). When the coil is placed against the scalp, it induces an e-field with mirror distribution of the coil current in the brain (Koponen *et al.*, 2015). According to Faraday's law, the magnetic field generates an e-field within the brain, which non-invasively modulates neural activity. In the targeted region with peak e-field, the stimulation causes the membrane potentials to depolarize. In previous studies, the most used coil shapes were round or a figure-of-eight shape. The annulus current produced by the round coil leads to an unfocused e-field. In contrast, the figure-of-eight coil produces a focally enhanced e-field, which is generated from the overlapping magnetic fields of two wings along the centerline of the coil (Roth *et al.*, 2007; Koponen *et al.*, 2018). A small circular coil can produce a relatively concentrated magnetic field, and the reduced numbers of windings on a small coil can only induce a magnetic field with low strength, thereby confining most of the effective stimulations to superficial tissues (Deng *et al.*, 2013; Roth *et al.*, 2013).

2.2.3 Line- versus electric-field navigated TMS

In previous navigation protocols, the maximum e-field was mostly assumed to be along the line through the center of and perpendicularly to the plane of the figure-of-eight shaped coils (Duffau, 2011; Sollmann *et al.*, 2016a). Therefore, at that time, the TMS coil was navigated to the place right over the targeting regions according to the subject's individual MRI reconstruction, which is called line navigated TMS (Ln-TMS) (Duffau, 2011; Sollmann *et al.*, 2016a). It was gradually realized the possibility of the line navigation leading to an inaccurate localization, which was later confirmed by a study comparing motor mapping results from the line- to e-field-navigated TMS (En-TMS) (Sollmann *et al.*, 2016a). The study demonstrated that line navigation tends to deviate stimuli to surrounding regions rather than the intended target when the coil is not in the supposed angle and/or position (Sollmann *et al.*, 2016a). Because when the plane of the eight-shaped coil is not parallel to the tangent plane centered on the contact point where the coil against the scalp (Figure 1), the different densities between the skull, skin, and air result in the refraction of the e-field. In detail, this study compared trains of stimuli

respectively navigated by an En-TMS system and an Ln-TMS system in patients with intracranial tumors. In this clinical study, those patients received preoperative motor mapping by both navigating TMS systems. Their differences in clinical applicability, workflow, and mapping results were analyzed. Motor mappings for each patient were performed in an alternating pattern of starting with either En-TMS or Ln-TMS system. The data showed that the number of motor-positive stimulation spots, the ratio of positive spots per overall stimulation numbers were significantly higher in En-TMS than that in Ln-TMS ; furthermore, the representative motor regions for upper- and lower-extremity localized by both systems were only partially overlapping (Sollmann *et al.*, 2016a). The designs of both TMS systems were certificated and applicable for mapping in patients with brain lesions. However, the differences between En-TMS and Ln-TMS should be carefully considered during clinical application in patients. In the current study, we only adopted En-TMS.

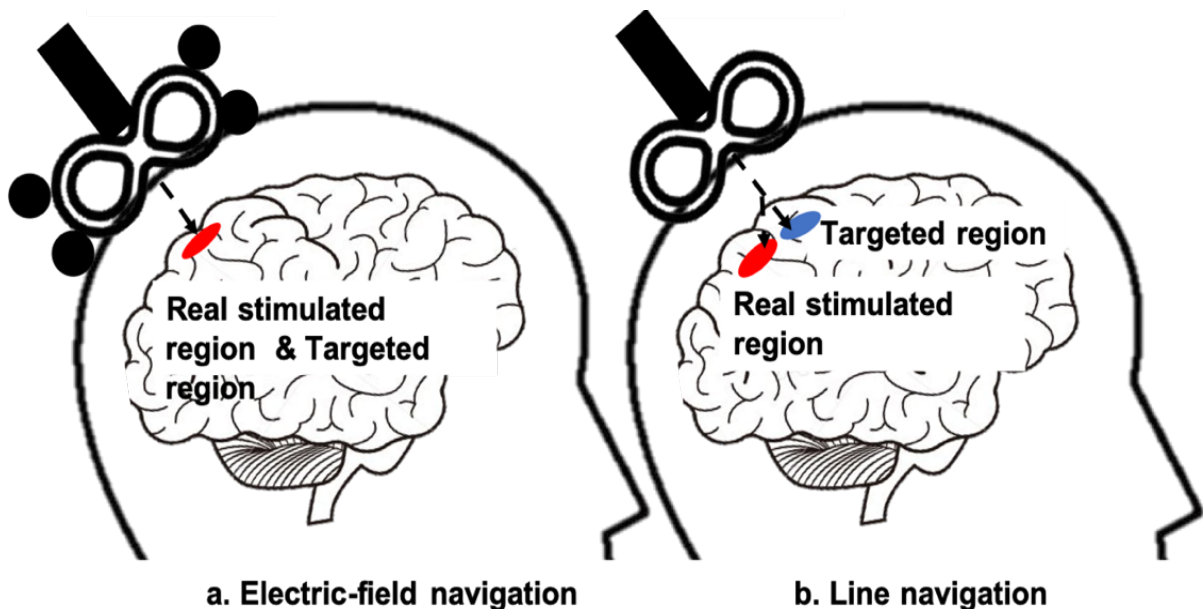


Figure 1. The difference between the En-TMS and Ln-TMS

Figure 1. The figure presents the difference between the two different navigation methods: a. Electric-field navigation: the actual stimulated area matches the target position. b. Line navigation: refraction occurs when the e-field passes through media of different densities, resulting in the misregistration between the actual stimulated area and the predefined target.

2.2.4 nTMS and individualized localization of language function

Facilitated by the development of navigation technology, nTMS as a non-invasive neurological function detection and intervention tool provides a new option for localizing function in neurosurgery. During the preparation for the surgery, nTMS enables doctors to detect and analyze alterations of functional representative areas' location and their relationships to tumor-induced functional deficits in patients. In nowadays clinical practice, it is mainly applied to test motor

and language functions (Najib *et al.*, 2011).

By nTMS this technique, the key regions controlling certain functions can be identified (Pascual-Leone *et al.*, 1999; Lioumis *et al.*, 2012b; Krieg *et al.*, 2014a; Sollmann *et al.*, 2015a; Sollmann *et al.*, 2017). In language mapping, this technique can induce a virtual lesion causing temporary language deficits classified into different categories, such as hesitations and semantic paraphasias, to localize their corresponding eloquent regions. From previous studies, the mapped regions by nTMS are well correlated with findings by intraoperative DES. The nTMS results could be used preoperatively to support the customized surgical plan (Picht *et al.*, 2013).

Awake surgery combined with intraoperative DES and intraoperative neuromonitoring (IONM) is the most widely used method in clinical practice to interact with brain functions directly. This method is still considered as the "gold standard" to test the applicability of other techniques in function localization currently (Talachchi *et al.*, 2013; Ottenhausen *et al.*, 2015; Sollmann *et al.*, 2018b), although some researchers have pointed out its shortcomings and the misconception (Borchers *et al.*, 2011). In 2013, Tarapore compared the functional localization results of nTMS to DES and reported that the specificity of nTMS was 90%, sensitivity 98%, positive predictive value (PPV) 69%, and negative predictive value (NPV) 99% (Tarapore *et al.*, 2013). In 2015, Ille *et al.* tested this method in 27 patients receiving preoperative nTMS mapping and DES test during tumor resection and found that the results of nTMS showed a sensitivity of 97%, a specificity of 15%, a PPV of 34%, and an NPV of 91% in comparison with mapped regions by DES (Ille *et al.*, 2015). Their studies confirmed the good consistency between nTMS and DES and demonstrated the reliability of nTMS language mapping, which can enhance the confidence of researchers and surgeons in clinical use. The preoperative nTMS mapping localizes language-related regions were used as regions of interest (ROI) in the tractography. These language-related fibers are then integrated into the navigation system (Krieg, 2017; Krieg *et al.*, 2017). During surgery, these predefined cortical and subcortical regions can facilitate the rapid identification of language-related regions by DES and suggest DES setups to elicit positive responses (Paiva *et al.*, 2012; Krieg, 2017).

2.2.5 nTMS-based DTI-FT for language function

nTMS currently has become one of the tools in clinical practice to identify language-related cortical regions. The stimulation of nTMS is used to elicit different kinds of naming errors on predefined targets on the hemisphere during an object-naming task. Regions, where stimuli induce errors are classified as language-positive nTMS points. Those nTMS points can also be used as ROI seeds to track subcortical language-related neural fibers called nTMS-based DTI-Fiber tracking (DTI-FT). It allowed further assessments of a single language-related tract or the whole brain networks. In previous studies, the method has been applied in preoperative preparation to detect language-related cortical and subcortical regions for estimating the risk of function loss during surgery. Moreover, it can be imported into the intraoperative navigation system as guidance during tumor resection. It is worth noting that this individualized functional analysis very conforms to the concept and principle of precision medicine.

TMS-based DTI-FT is based on the deterministic algorithm using individually localized ROIs

on language functions. The feasibility and reliability of nTMS-based DTI-FT have been confirmed in previous studies (Frey *et al.*, 2012; Raffa *et al.*, 2016; Sollmann *et al.*, 2016b; Sollmann *et al.*, 2018c). Raffa's study compared it with the standard atlas-based DTI-FT method and found that nTMS-based DTI-FT was analyzed under higher FA values and led to more successful visualization of cortico-subcortical connections and increased its reliability (Raffa *et al.*, 2016). Hence, it was suggested that the nTMS-based approaches were superior to the atlas-based methods (Raffa *et al.*, 2016).

This technology directly uses the cortical regions related to the language function as seed points while not depending on the operator's understandings and experience on cerebral functional anatomy, thereby avoiding artificial errors caused by subjective factors. Negwer's study compared the results from anatomical methods and nTMS-based DTI-FT for localizing language-related fibers and concluded that the latter is advantageous in repeatability for clinical application (Negwer *et al.*, 2017b). In Raffa's article, the same conclusion was proposed (Raffa *et al.*, 2017). In summary, the DTI-FT of nTMS positive points can better indicate the functional distribution of the brain areas around the tumor before surgery, which can help doctors optimize the tumor resection plan and reduce the size of the surgical bone window. Hence, it leads to better protection on the basic function (Negwer *et al.*, 2017b; Raffa *et al.*, 2017).

In a subsequent study by Negwer *et al.*, the protection of language-related nerve bundle branches before and after surgery was compared. It was found that there was a positive correlation between the tracked fiber volume loss by nTMS-based DTI-FT and the clinical prognosis of language function (Negwer *et al.*, 2018).

2.3 Language-related Fiber Tracts and Their Functions

The common parameters used in DTI fiber tracking (DTI-FT) are fractional anisotropy (FA), fiber length (FL), and angulation. Fractional anisotropy (FA) is a scalar value between zero and one that describes the degree of anisotropy of a diffusion process (Basser and Pierpaoli, 1996). With different setups of the above-mentioned tracking parameters, the DTI-FT using ROI from the pre-defined eloquent cortex or subcortical regions is a potential method to identify the functional-related structures and their organizations in the brain (Burgel *et al.*, 2009; Li *et al.*, 2013; Negwer *et al.*, 2017b). This method is widely used for detecting motor function (Krieg *et al.*, 2012a; Niu *et al.*, 2016; Sollmann *et al.*, 2018c) and language function in daily clinical practice (Sollmann *et al.*, 2016b).

2.3.1 Language-related neural tracts

In previous studies, DTI was combined with other imaging methods or functional localization techniques, mostly fMRI and nTMS, to analyze the relationship between intracranial neural tracts and different aspects of language function. The following section outlines a brief summary for the roles of each intracranial tract concerning language function, including the arcuate fascicle (AF), superior longitudinal fascicle (SLF), inferior longitudinal fascicle (ILF), uncinate fascicle (UF), fronto-occipital fascicle (FoF), commissural fibers (CF), corticonuclear tract

(CNT), corticothalamic fibers (CtF), and arcuate fibers (ArF):

- a) **AF**: the combination of neuropsychological inference and comprehensive language tests with DTI analysis demonstrated that the involvement of the AF was contingent upon the demands of different components of language function (Rolheiser *et al.*, 2011; Skorpil *et al.*, 2011).
- b) **SLF**: the SLF facilitates the formation of a bidirectional neural network necessary during language processing (Oliveira *et al.*, 2017). The trajectory and connectivity of the SLF are related to other language pathways as well as the superior parietal lobule (Kamali *et al.*, 2014). When Nakajima *et al.* separated the SLF into dorsal and ventral parts for investigating their respective functions, they demonstrated that the dorsal SLF is involved in visuospatial attention and motor control. In contrast, the ventral SLF was related to language-related networks, auditory comprehension, and articulatory control in the left hemisphere (Nakajima *et al.*, 2019).
- c) **ILF**: Green *et al.* demonstrated the significant correlations detected between measurements of the reading process and properties of the left ILF in adults (Green *et al.*, 2013). The study on the later second language learners found that the FA of ILF increased and was correlated with their ages (Rossi *et al.*, 2017).
- d) **UF**: A robust and replicable relationship was found between the UF and associative learning and memory in the study by Metoki *et al.* (Metoki *et al.*, 2017), which potentially modulated language processing.
- e) **FoF**: FoF was suggested to be correlated with the status of speaking function in patients with left-sided perisylvian gliomas not only at preoperative and postoperative phases, but also at the follow-up phase (Ille *et al.*, 2018).
- f) **CF**: Cognition relies mostly on the CF tracts (Rossi *et al.*, 2012), which is the foundation of interaction with surrounding circumstances.
- g) **CNT**: Functional organization in CNT trajectory to motoneurons to control lower facial muscles responsible for correct pronunciation (Meyer *et al.*, 1994).
- h) **CtF**: Based on the recent literature by Crosson *et al.* on aphasia and thalamic activity on neuroimaging, regarding its structure and function, it is concluded that the CtF joined corticothalamic and/or thalamocortical mechanisms impact language processing (Crosson, 2013).
- i) **ArF**: In Negwer *et al.*'s study, ArF has been found in the nTMS-based DTI-FT (Negwer *et al.*, 2017b). However, its role in language processing has not been discussed in detail. The current study investigates the ArF and its role in language processing.

However, in the previous studies, neither the relationship between the subcortical fibers is clearly elaborated, nor the relationship between these tracts and different categories of linguistic errors induced by nTMS. This will be investigated in the current study.

2.3.2 Language-related dorsal and ventral streams

Previous investigations have found that a single neural tract may not be enough to maintain

language function, indicating that the anatomical and functional basis of language function may involve a network-based system composed of multiple cortical regions and subcortical connections (Hickok and Poeppel, 2007; Li *et al.*, 2015; de Heer *et al.*, 2017). Based on these studies, the "dual-stream hypothesis" was proposed to describe the language-related subcortical organization. Fibers were separated into dorsal and ventral streams based on their anatomical locations (Hickok and Poeppel, 2004; Kummerer *et al.*, 2013; Fridriksson *et al.*, 2016; Dittinger *et al.*, 2018). These two streams are considered processing information synergistically but with the anatomical distinction between a dorsal frontoparietal stream supporting a form-to-articulation pathway and a ventral temporal–frontal stream supporting a form-to-meaning pathway (Rauschecker and Scott, 2009; Friederici, 2012a; Friederici and Gierhan, 2013; Fridriksson *et al.*, 2016).

The dorsal stream comprises two subparts: one connecting the temporal cortex with the premotor cortex via the SLF, while the other connecting the temporal cortex with Broca's area via the AF (Friederici, 2011, 2012b; Rauschecker, 2012; Friederici and Gierhan, 2013). In the study by Hillis *et al.*, the stroke patients with lesions in left SLF/AF presented a poorer performance in the object naming task (Hillis *et al.*, 2018). It was supported by the investigation by Liégeois *et al.*, in which it demonstrated that the lesion to the dorsal stream would lead to speech disorders and speech delay (Liegeois *et al.*, 2019).

In contrast, higher-level comprehension of language is mediated by the ventral stream connecting the middle temporal lobe and the ventrolateral prefrontal cortex (Saur *et al.*, 2008; Rauschecker and Scott, 2009; Rauschecker, 2012). It consists of the fronto-occipital fascicle (FOF), uncinate fascicle (UF), and inferior longitudinal fascicle (ILF). The ventral stream plays a key role in auditory object recognition, including the perception of both vocalizations and speeching (Hickok and Poeppel, 2004; Rauschecker, 2012).

Changes in the dual streams based on the different error types identified by the nTMS language mapping have not been studied and analyzed before. Investigating the dual-stream hypothesis via TMS-based DTI-FT analysis can provide a new perspective on the organization of language-related brain structures, thereby further deepening the understanding of language processing.

2.4 Aim of the Current Study

In the prior studies, 6 types of linguistic errors are identified in nTMS language mapping and used for analysis, consisting of no responses, performance errors, hesitations, neologisms, phonological paraphasias, and semantic paraphasias (Sollmann *et al.*, 2015c; Krieg *et al.*, 2016; Sollmann *et al.*, 2018a). Those errors have been well defined and accepted in the neuroscientific domain. In previous articles on TMS language mappings, the brain regions related to different errors are commonly combined as a single ROI to track the language-related fibers. However, until now, the difference in the tractography corresponding to different naming errors induced by stimulation has not been clarified. Against this background, the current study was conducted to investigate the following foci/aims:

- (1) Assessing the relationship between specific error types and their corresponding subcortical language-related pathways;

- (2) Searching for potential dominant fibers/tracts in certain linguistic errors;
- (3) Evaluating whether the nTMS-based DTI-FT using ROI of one single error category was superior to the ROIs defined by all errors;
- (4) Investigating whether the ventral stream and the dorsal stream contribute differently to the linguistic function.

3. MATERIALS AND METHODS

3.1 Ethics

All our studies were performed following the ethical standards published in the 1964 Declaration of Helsinki and its later amendments after receiving approval from the local institutional review board (registration number: 2793/10). All subjects provided their informed consent before being enrolled.

3.2 Patients and Study Inclusion

40 subjects with left-hemispheric perisylvian tumors receiving tumor resections in our neurosurgical department were enrolled in the current study between 2016 and 2018. Patients had to meet the following inclusion criteria:

- (1) Above 18 years old;
- (2) Written informed consent;
- (3) Tumor located within the left-hemispheric perisylvian regions.

The exclusion criteria were defined as follows:

- (1) Other neurological or psychiatric disorders besides the brain tumor, including Schizophrenia, congenital hydrocephalus, etc.;
- (2) General nTMS or MRI exclusion criteria (e.g., with cochlear implants, claustrophobia);
- (3) Global aphasia, rendering it impossible to conduct preoperative language mapping;
- (4) Impaired comprehensions and inability to cooperate during the test, for example, consciousness disorders, mental retardation, etc.

3.3 Study Design and Clinical Examination

During the preoperative preparation, all patients underwent the basic clinical examination and assessments on language performance. Their sensory, coordination, muscle strength, and cranial nerve function were measured according to the standardized protocol. Furthermore, the Karnofsky performance status (KPS) score was assessed (Peus *et al.*, 2013). Any presence of epileptic seizures and antiepileptic drug intake at the time of testing were documented. After resection, the clinical examinations were repeated daily during their hospitalization and follow-up examinations in the hospital every 3–12 months, depending on the pathology of the tumor and the patient's recovery. The workflow of this experiment is presented in the figure below (Figure 2).

The dominant hand was estimated by the neuroscientist using the Edinburgh Handedness Test (Futai, 1977).

The British Medical Research Council (BMRC) scale was used to evaluate the muscles' strengths. It was recorded as 5/5 when no motor deficits were manifested and scored with <5/5 when presenting any paresis. This clinical assessment was conducted repeatedly right after the operation and during follow-up in the clinic every 3-12 months after discharge.

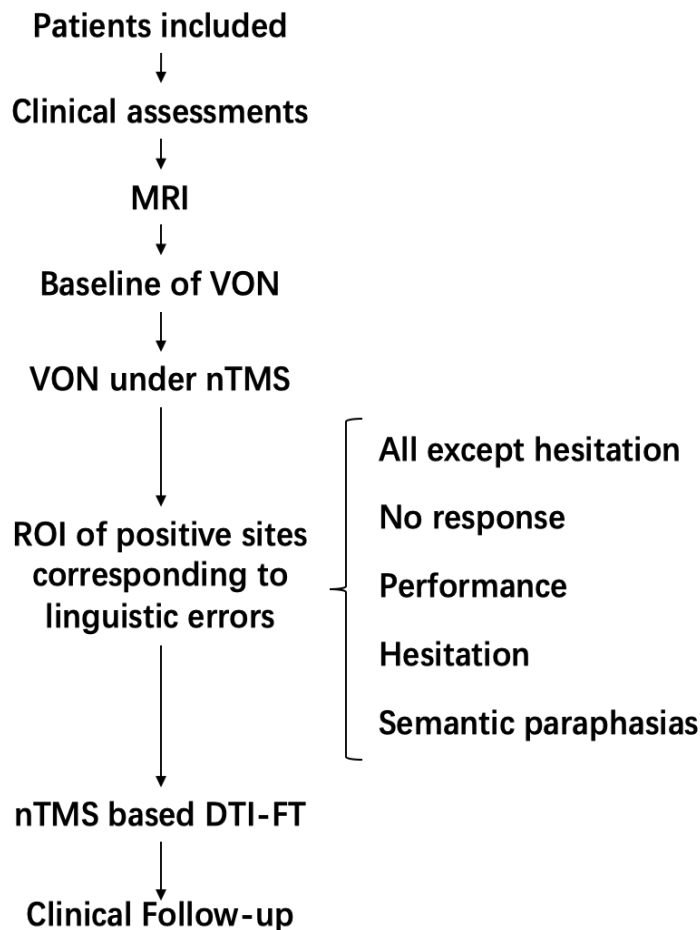


Figure 2. Workflow of the current study

Figure 2. This figure presents the design and process of the current study.

VON: Visual Object Naming.

The AAT was used as a measurement for language deficit conducted by our trained neurosurgeon with more than 3 years of experience. The language levels were set into 4 grades, as follow (Huber *et al.*, 1984; Wacker *et al.*, 2002; Sollmann *et al.*, 2015b; Kelm *et al.*, 2017; Sollmann *et al.*, 2018b):

- (1) Grade 0: no deficits;
- (2) Grade 1: mild deficits, normal speech comprehension and/or conversational speech with slight amnesic aphasia, adequate communication ability;
- (3) Grade 2: medium deficits, minor disruption of speech comprehension and/or conversational speech, adequate communication ability;

- (4) Grade 3: severe deficits, major disruption of speech comprehension and/or conversational speech, clear impairment of communication ability.

Regarding the language status, the following pre-defined binary categories were used to classify the recovery level (Kelm *et al.*, 2017; Sollmann *et al.*, 2018b):

- (1) Transient surgery-related deficits: any new or worse deficits postoperatively due to surgery, which will recover to the same status as their preoperative language performance or even better;
- (2) Permanent surgery-related deficits: any new or aggravated deficits in the postoperative phase due to surgery, which did not relieve within the regular follow-up interval.

All included patients underwent preoperative MRI and nTMS language mapping before surgery. After that, nTMS-based DTI-FT for subcortical language-related pathways was individually performed. The images derived from MRI, nTMS language mapping, and nTMS-based DTI-FT were combined to plan the resection preoperatively and made available for the intraoperative guidance.

3.4 Magnetic Resonance Imaging

A standardized imaging protocol was routinely implemented for all patients with cerebral tumors in our department using a 3 Tesla MRI scanner (Achieva, Philips Medical Systems, Best, The Netherlands). Four sequences from the protocol were used in the current study, including:

- (1) a three-dimensional (3D) fluid-attenuated inversion recovery (FLAIR) sequence (TR/TE: 4800/277ms, 1mm³ isovoxel covering the whole head);
- (2) a 3D T1-weighted gradient-echo sequence (TR/TE: 9/4 ms, 1 mm³ isovoxel covering the whole head);
- (3) an enhanced 3D T1-weighted gradient-echo sequence with the administration of a contrast agent (Dotagraf, Jenapharm, Jena, Germany);
- (4) a DTI sequence (TR/TE 5000/78 ms, voxel size of 2 × 2 × 2 mm³, 32 diffusion gradient directions);

The scans above were collected preoperatively. The preoperative 3D T1-weighted gradient-echo sequences were used to assess the volumetric impacts of the tumor size through IntelliSpace Portal (version 9.0; Philips Healthcare, Best, The Netherlands).

Within the first 48 hours subsequent to the surgery, postoperative MRI scans were conducted using the same sequences as in the preoperative phase, furthermore, including a T2*-weighted imaging. After discharge, further MRI scanning was carried out during their follow-up.

3.5 Language Mapping by nTMS

3.5.1 Registration

Preoperative language mapping was performed with the Nexstim eXimia NBS system (version 4.3; Nexstim, Helsinki, Finland). The contrast-enhanced T1-weighted gradient-echo imaging was imported to the system and used to reconstruct the 3D brain for later navigating the stimulation on targeted cerebral regions during the mapping process. A head tracker was attached to the patients' forehead to track the movements and navigate the location.

The crux of the helix from both ears and the nasion were used as landmarks to register the personal heads to their 3D reconstructed images. Then nine scalp areas around the head automatically defined by the system were applied to further correcting the registration. The system only allowed for later processing when the mismatch of registration was under 5 mm.

3.5.2 Rough mapping

The electrodes were attached to the tendon and belly of muscles on the contralateral upper extremity, including Abductor pollicis brevis muscle (APB), Abductor digiti minimi (ADM), Flexor carpi radialis muscle (FCR), and ipsilateral APB to record the motor evoked potential (MEP) and latency between the stimulation and muscle reaction. Each MEP was composed of the takeoff, peak, trough, and recovery phases. The correct MEP latency is defined as the takeoff time within between 18~25ms, and the positive MEP amplitude was defined by the absolute difference between the peak and trough ($\geq 50\mu\text{V}$).

During rough mapping, the direction of stimuli was oriented to be perpendicular to the gyrus. The rough mapping was for two purposes: one was to have a rough view of the distribution of the motor regions, and the other one was to identify the hand motor hotspot. The hotspot was defined as the target that generated the highest amplitude of MEP under the lowest stimulation intensity (Wang *et al.*, 2020).

The single-pulse stimulation setups were as follow:

- (1) Intensity: the stimulation started with 30% intensity of the maximal coil output. When no MEP induced after 5 stimuli, the intensity was increased to 5%;
- (2) Stimulus interval: 1.5s.

The stimuli were outputted targeting the motor function-related cortical regions in the dominant hemisphere, especially the handknob regions (Figure 3).



Figure 3. Rough mapping on hand knob

Figure 3. This figure presents the stimulus (yellow match-shaped sites) on the handknob area during TMS rough mapping.

3.5.3 Angulation

On the hotspot, the angulation of stimulus was tested to find the most sensitive adjustment of e-field direction, which was later applied in the setup of the stimulation for measuring the resting motor threshold (rMT). The angulation was measured following steps as below:

- (1) Firstly, the coil outputted 5 stimuli on the hotspot at the angulation suggested by the system (Figure 4.a).
- (2) Secondly, the coil outputted 5 stimuli at each of the other angulations (Figure 4.b and 4.c).
- (3) Thirdly, the MEPs from each angulation were compared to find the angulation of the coil inducing the best response of MEP. This MEP corresponding muscle was used to measure the rMT.

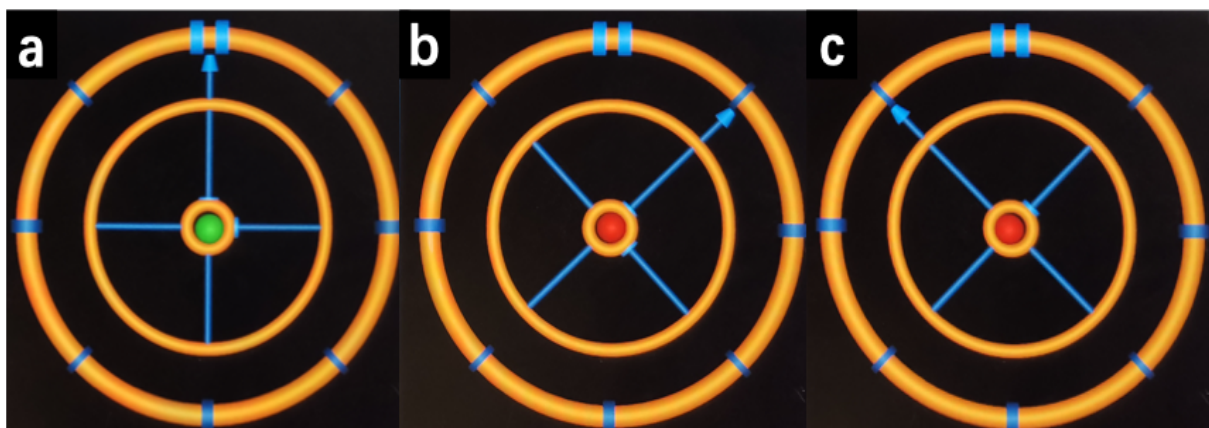


Figure 4. Angulation test process.

Figure 4. This figure presents the stimuli outputted at each direction to test the best angulation of the coil. 4a) the angulation is perpendicular to the brain gyrus; 4b) the angulation is at +45° to the direction used in 4a; 4c) the angulation is at -45° to the direction used in 4a.

3.5.4 Resting motor threshold determination

The most sensitive MEP channel and angulation were used to determine the resting Motor Threshold. The individual rMT was defined as the lowest intensity required to evoke a positive MEP (amplitude $\geq 50\mu\text{V}$, latency within 18~25 ms) in the predefined channel from the relaxed upper extremity muscles in at least 5 out of 10 consecutive trials (Groppa *et al.*, 2012). The nTMS system automatically decreased or increased the intensity according to the MEP amplitude until the stimulus intensity that met the rMT definition was detected (Figure 5a and 5b).

The screenshot shows a software window titled "Motor Threshold". It is divided into several sections:

- Process parameters:**
 - Starting parameters:** Amplitude threshold is set to 50 μV , and Starting intensity is set to 4 %.
 - Ending parameters:** Max number of counted stimuli is set to 30 (checked), and Motor Threshold estimate +/- is set to 2.5 (checked).
- Muscle information:** EMG channel is set to 1. EMG (dropdown menu), and Muscle is set to EMG (text field).
- Researcher:** An empty text input field.
- Description:** A text area containing "Motor Threshold for EMG".

At the bottom of the window are two buttons: "Start" and "Cancel".

Figure 5a. Setup interface for rMT definition

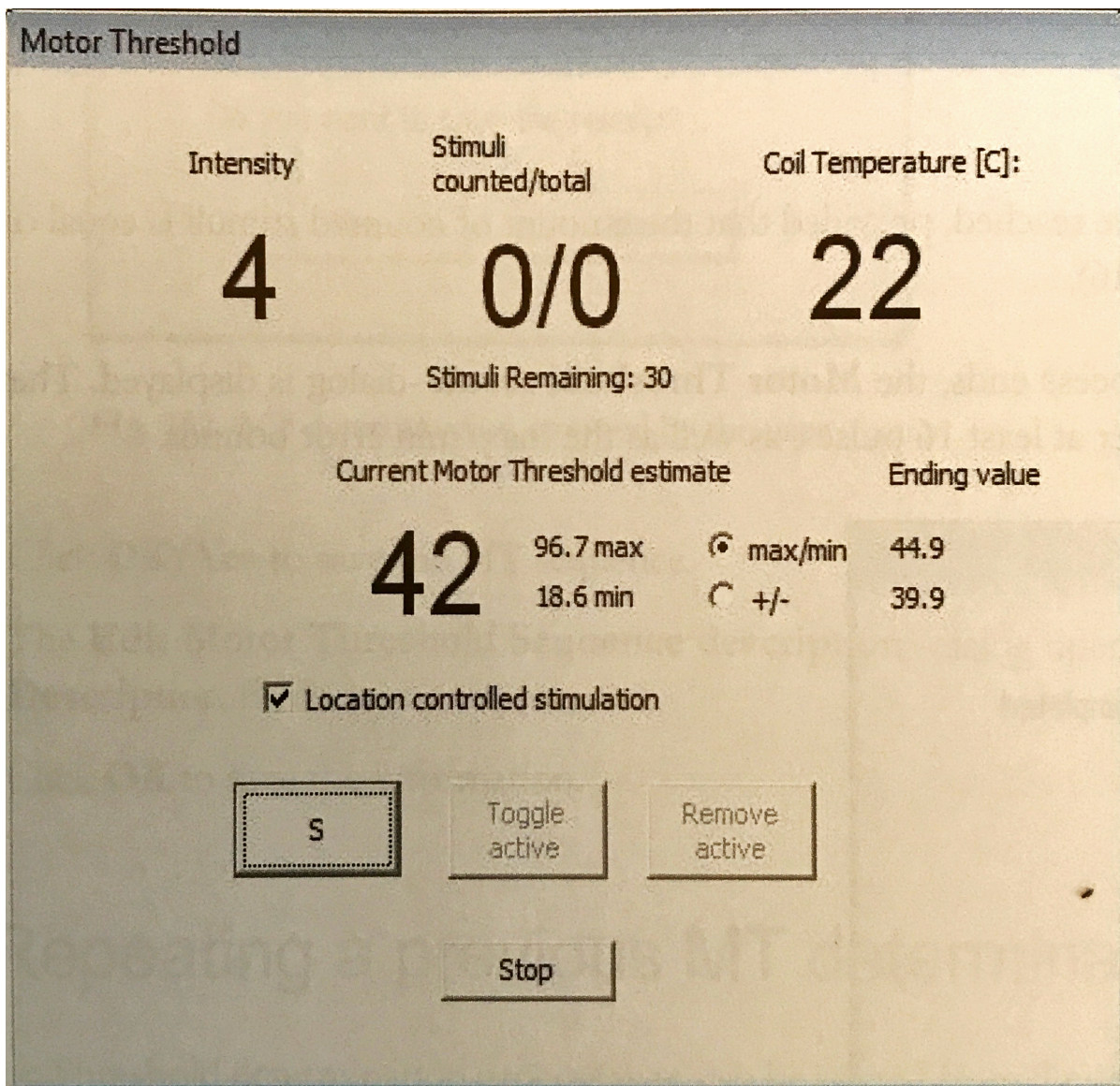


Figure 5b. Interface of rMT definition when stimuli outputted on the brain

Figure 5. This figure shows that the nTMS system automatically decreased or increased the intensity according to the MEP amplitude until the stimulus intensity that met the rMT definition was detected (Figure 5a and 5b).

3.5.5 Cortical parcellation system template

Due to the distorted cerebral structures caused by a tumor, the automatic parcellation is inaccurate in identifying the nTMS targets. A skilled neuroscientist and a neurosurgeon artificially marked the stimulating targets on the dominant hemisphere according to the template of cortical parcellation system (CPS) (Figure 6), which had been adopted in the previous studies (Sollmann *et al.*, 2015d; Sollmann *et al.*, 2016b; Krieg *et al.*, 2017; Negwer *et al.*, 2017b). In this system, all potential language-related brain regions in the hemisphere are divided into 21 regions with 46 stimulation targets, on which the corresponding nTMS stimulation targets are set. This target setting based on individual MRI can better subdivide the brain structures, thereby improving the accuracy of stimulation.

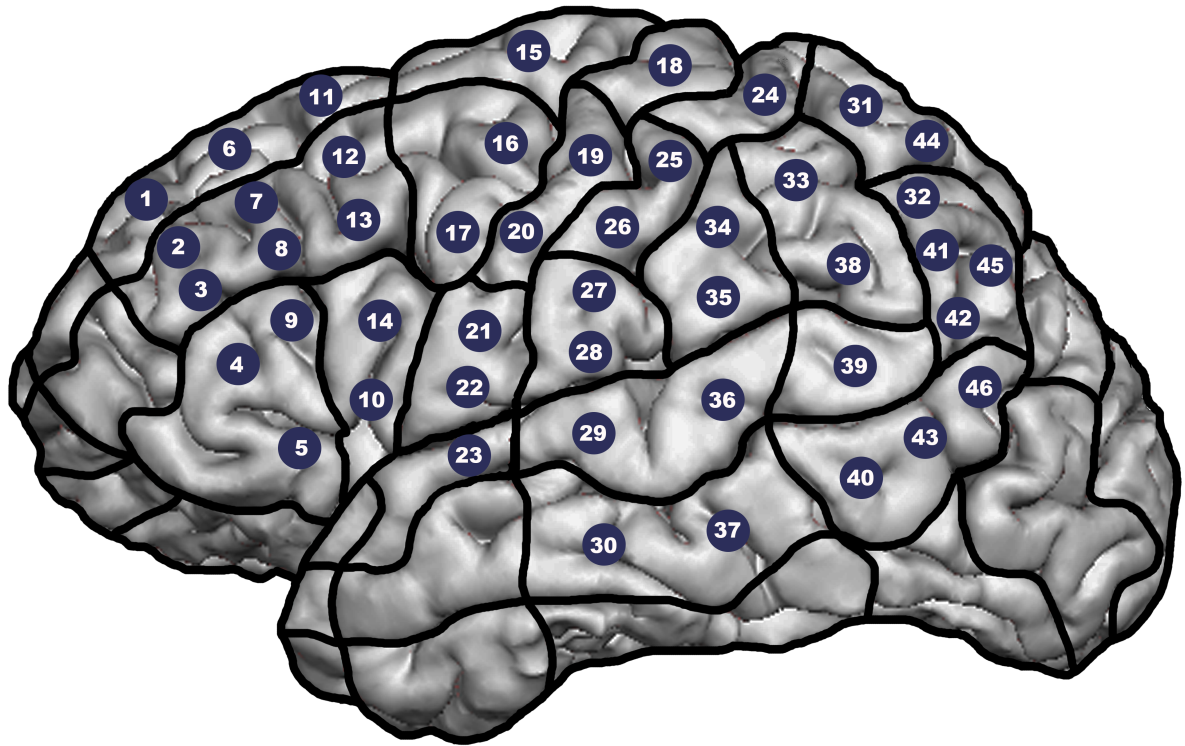


Figure 6. CPS template with 46 targets on the cortex for nTMS language mapping.

Figure 6. This figure presents the 46 stimulation targets set on the hemisphere according to the CPS template.

3.6.6 Language mapping process

Before the test started, it was necessary to inform and confirm that the patient understands the vocal objects naming (VON) examination process correctly. If the patients were unable to communicate in any language or understand the conversation, the test would be abolished. After confirming patients' conditions feasible for nTMS language mapping, 3D structural reconstruction with 46 targets set according to CPS template in the Nexstim eXimia NBS system (version 4.3; Nexstim, Helsinki, Finland) was used in the navigation system to guide the stimulation coil in the correct angle and position above the targeted regions during the mapping process.

Firstly, the patients were asked to take a semi-recumbent position on the examination chair. The screen displaying objects for the naming task was about 30 - 50 cm away from the patient's eyes to guarantee that the pictures are clear to the patients. Three important criteria were ensured:

- (1) The patient felt comfortable when in the examination position.
- (2) The patient could clearly recognize the picture displayed on the screen.
- (3) The patient felt comfortable or tolerable when stimulated by the TMS.

After confirming the above-mentioned points, the test process could be started.

All objects drawn only in black lines with a white background were presented on the screen (Figure 7). The display time was 700ms with an interval of 2500ms, which would be adjusted accordingly to acquire the patients' best performance. The patient was asked to name the items in German (without the article/determiner) when they are presented on the screen during the task.



Figure 7. Objects for naming task.

Figure 7. This figure presents example objects used in the naming tasking. During the task, those objects are regularly presented on the screen (in Figure 8) directly facing subjects.

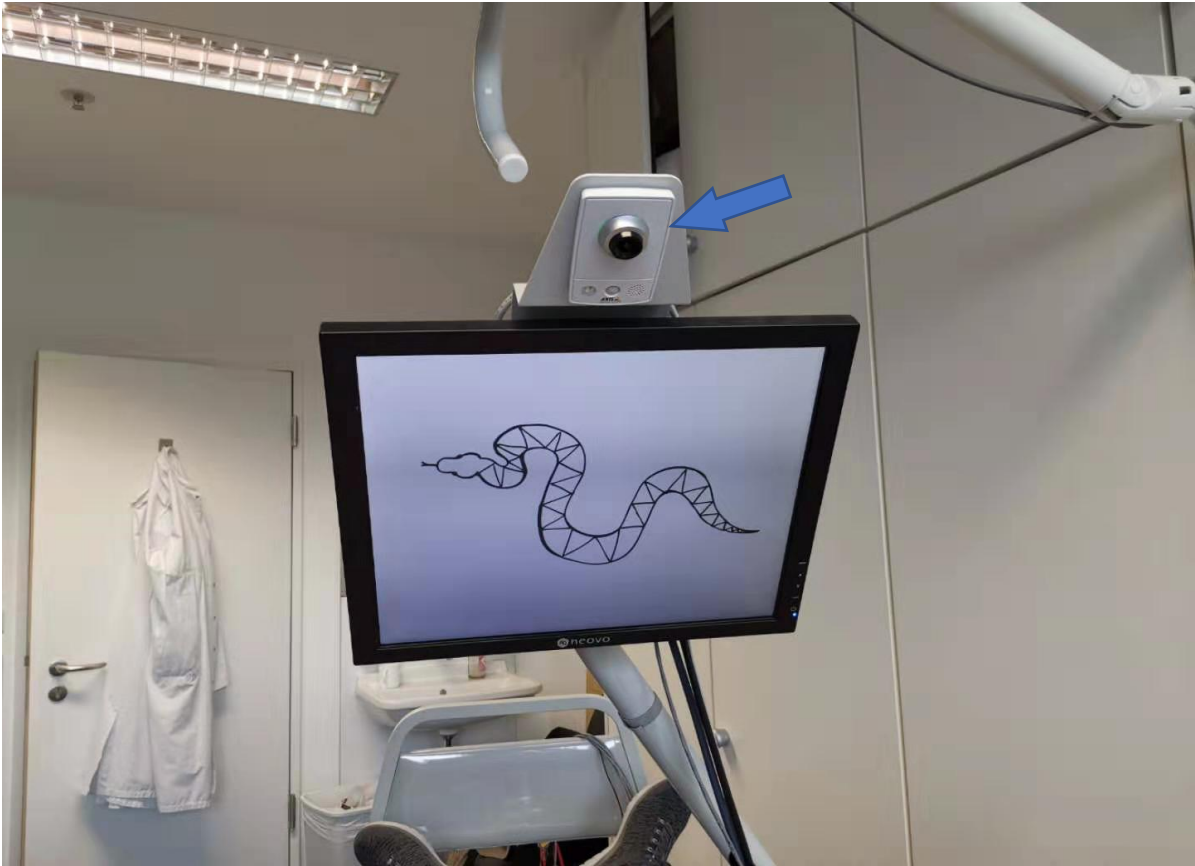


Figure 8. Video recorder.

Figure 8. In the figure, the blue arrow on the picture points at the camera device, which records the subjects' performance in object naming task. The baseline performance without stimulation is recorded to compare with the record of object naming performance with stimulation.

For the language test, the patient was required to perform VON tasks without stimulation twice for getting the solid baseline performance and once with stimulation for mapping the language-related brain regions. The high-definition (HD) camera was located at the top of the screen (Figure 8), facing the patient directly and recording the patient's performance during the VON task in real-time. All the patient's responses were automatically sorted to match their corresponding object picture and nTMS stimulus, and the Nexstim system also recorded the response time.

The first baseline VON task was to familiarize the patient with the task's execution process and objects on the pictures. Pictures were excluded when their objects were unfamiliar or confusing to the patient. For example, when a patient named the third object in the first row of Figure 7 (it may be called a "Weinglas," or "Glass," or "Becher"), or showed a long hesitation in naming this object, or named the picture differently when it presented again, then the object picture would be deleted. In some patients, the intracranial tumor may cause slow speech and insufficient energy. When 8 out of 10 objects could not be named in time by patients, the display time or/and interval time was extended at 500ms. The purpose of the above-mentioned adjustments of object pictures and stimulation parameter settings was to guarantee a stable performance in the second session.

Then, the baseline VON task was repeated to confirm the performance of the patient in the first baseline task. Parameters and object pictures adjusted in the first baseline task were applied in the second baseline task as well (Lioumis *et al.*, 2012b; Picht *et al.*, 2013; Krieg *et al.*, 2017). After the second baseline test, if the patient felt tired, he or she could rest for 10-15 minutes, and the water was provided to patients.

In the following stimulation session, patients were asked to conduct the VON task under repetitive nTMS stimulation. All object pictures and parameters were the same as those used in the base-line test. Each target would be stimulated 6 times. Stimulation parameters were set as below (Krieg *et al.*, 2017):

Strength: 100% rMT;

Frequency: 5Hz;

Pulse/train: 5 pulses per train.

Stimuli were outputted on predefined targets during the VON task. The stimulus was synchronized with the picture displaying. The nTMS coil was navigated by the Nexstim system to ensure that the electrical field on the targeted regions was correctly positioned and outputted consecutively.

In the posthoc analysis, videos of task performance recorded in the second baseline and task performance under-stimulation are compared by the experienced TMS technician and

neurosurgeons to find the naming errors and classify them into 6 types according to the definitions as follow (Corina *et al.*, 2010; Lioumis *et al.*, 2012b; Picht *et al.*, 2013; Hernandez-Pavon *et al.*, 2014; Krieg *et al.*, 2017; Hauck *et al.*, 2018) :

- (1) No responses: the patient completely failed to make any verbal response to the object presented on the screen;
- (2) Performance errors: articulatory errors, specifically form-based distortions that are spluttered or inaccurate;
- (3) Hesitations: delayed naming onset. Compared with the performance in the baseline, there is a significant delay in verbal reaction, and may be accompanied with a hesitant expression before pronunciation;
- (4) Neologisms: form-based naming errors due to using possible but non-existent words. These errors are distinguished from performance errors, which are the incorrect articulatory expression of the existing word;
- (5) Phonological paraphasias: unintended substitution, insertion, deletion, or transposition leading to the phonemic modification of the target words. Phonemic paraphasia, also known as literal aphasia, refers to replacing words with non-words that retain at least half of the segments and/or the number of syllables of the intended word.
- (6) Semantic paraphasias: also known as verbal paraphasia, the target words are substituted by semantically related or associated words, such as saying “Heimat” or “Villa” instead of “Haus.”

By comparing language performance, the type of patient's language error can be determined, and the corresponding TMS stimulation location was determined. Thereby, functional errors can be directly linked to corresponding regions in the cortex. Notably, 4 types of linguistic errors are mostly detected in nTMS language mapping according to previous studies consisting of no responses, performance errors, hesitations, and semantic paraphasias, which were used to analyze the mapping of respective single error category in the current study (Sollmann *et al.*, 2015c; Krieg *et al.*, 2016; Sollmann *et al.*, 2018a). Based on that, the targets corresponding to all errors except hesitations (including no responses, performance errors, neologisms, phonological paraphasias, and semantic paraphasias together) and single error (respectively, no responses, performance errors, hesitations, and semantic paraphasias) were identified in nTMS mapping data and exported as a single file respectively, which contained objects in three depths (15 mm, 20 mm and 25 mm) from each target in the format called Digital Imaging and Communications in Medicine (DICOM). This imaging format is consistent with the data format in the picture archiving and communication system (PACS) for the compatibility and accessibility of the mapping results. The platform of Brainlab software (Brainlab iPlan Net server, version 3.0.1, Brainlab AG) connected to the PACS system enabled the achievement of further data processing and visualization of language function-related stimulation targets. The DICOM file containing the function-related stimulation targets obtained above was uploaded to the server through this system. Then the data was able to be analyzed and processed on the iPlan platform.

Each of the following categories of language errors corresponding to the contrast-enhanced T1-weighted gradient-echo imaging file with its related stimulation targets was set as the seed region for later nTMS-based DTI-FT in the iPlan platform:

- (1) All errors except hesitations corresponding stimulation targets;
- (2) No responses corresponding stimulation targets;
- (3) Performance errors corresponding stimulation targets;
- (4) Hesitations corresponding stimulation targets;
- (5) Semantic paraphasias corresponding stimulation targets.

3.7 nTMS-based DTI-FT

All tractography and analysis steps were conducted on the Brainlab iPlan Net server (version 3.0.1, Brainlab AG, Munich, Germany).

Each of the five DICOM files exported from the Nexstim system was based on the T1-weighted gradient-echo imaging for registering in the same space. Then, these targets from different categories, respectively contained in their corresponding DICOM files, were used to construct the ROI seeds in 3 depths (15 mm, 20 mm, and 25 mm to the scalp) in the brain. The 5 ROI seeds represent 5 linguistic errors: all errors except hesitations, no responses, performance errors, hesitations, and semantic paraphasias.

The algorithm used for the tractography was deterministic fiber tracking based on the ROI seed mentioned above. The ROI seeds were separately fused to the preoperatively acquired enhanced 3D T1-weighted gradient-echo image to register their spatial locations. Then DTI files fused to the 3D T1-weighted gradient-echo image, during which the eddy current correction was applied to reduce distortions. As a result, the DTI and the seeds were in the same space as the structural image.

Regarding the tractography setup of the fractional anisotropy (FA), Sollmann et al. proposed the method of quartile FA as the thresholds, which was applied in the current study (Sollmann et al., 2016b). In the process of determining the individual FA threshold (FAT), 2 steps were conducted in sequence:

- (1) The fiber length (FL) threshold was set to 110 mm, and the FA was increased stepwise at 0.01 until displaying no fiber courses (Frey et al., 2012; Sollmann et al., 2016b);
- (2) This FA value decreased by 0.01 was regarded as the 100% FAT (Frey et al., 2012; Sollmann et al., 2016b).

This FAT value corresponded to visualization of the minimum fiber course (Frey et al., 2012; Sollmann et al., 2016b). Besides 100% FAT, 75% FAT and 50% FAT were also calculated and used as thresholds for the following DTI-FT.

The FT in the current study was purely based on nTMS language mapping data under respective setup with FA and FL (Sollmann et al., 2016b; Negwer et al., 2017a). The fixed FA and individualized quartile FAT were both applied to FT thresholds, as follow:

- (1) FA = 0.10, FL = 100 mm;
- (2) FA = 0.15, FL = 100 mm;
- (3) FA = 100% FAT, FL = 100 mm;
- (4) FA = 75% FAT, FL = 100 mm;
- (5) FA = 50% FAT, FL = 100 mm.

Then, each of the 5 ROIs was used for DTI-FT under each of the 5 FA setups. Therefore, a total of 25 kinds of tractography were conducted for each subject.

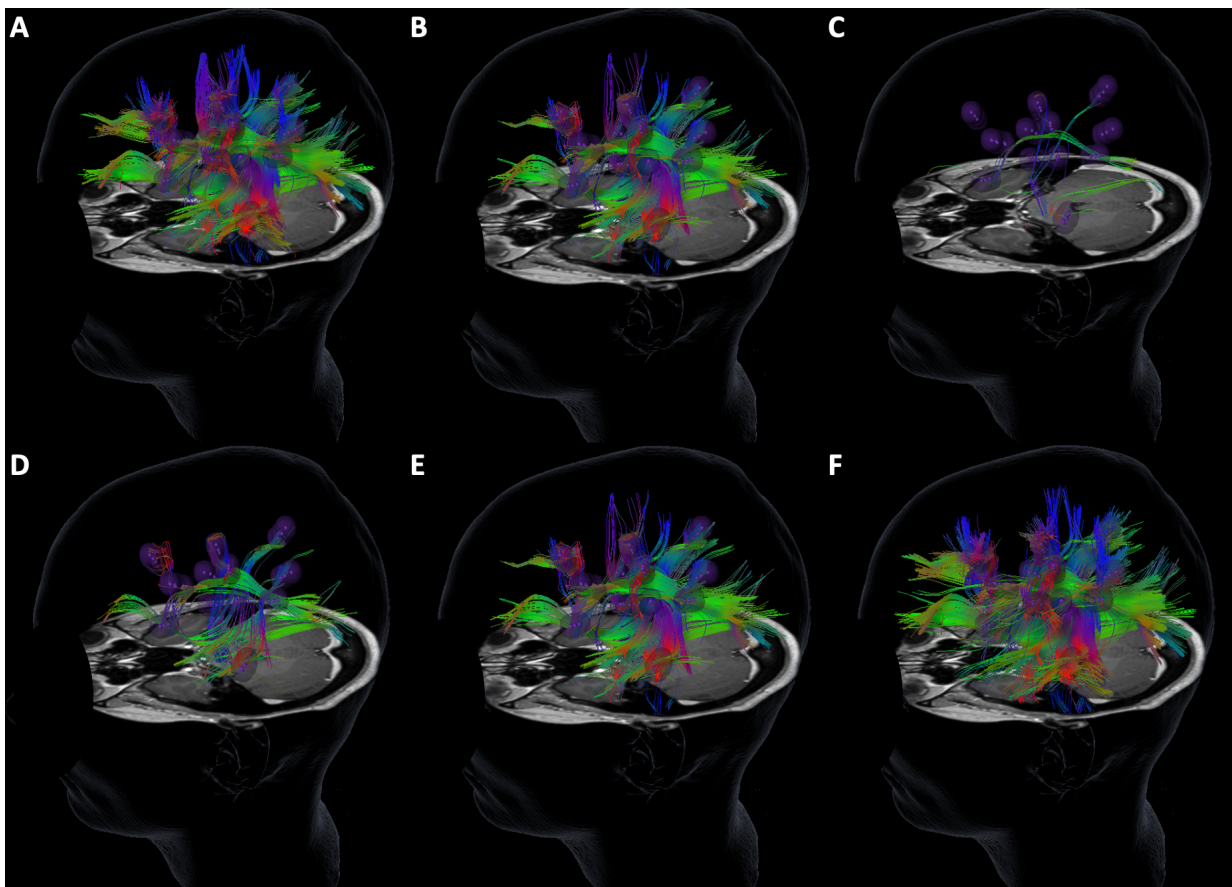


Figure 9. FT under each setup of FA thresholds.

Figure 9. In this figure, the FL threshold is 100 mm. For the seed, the category “all errors except hesitation.” is used here. A. the FA is 0.1; B. the FA is 0.15; C. under 100% FAT; D. under 75% FAT; E. under 50% FAT; F. under 25% FAT.

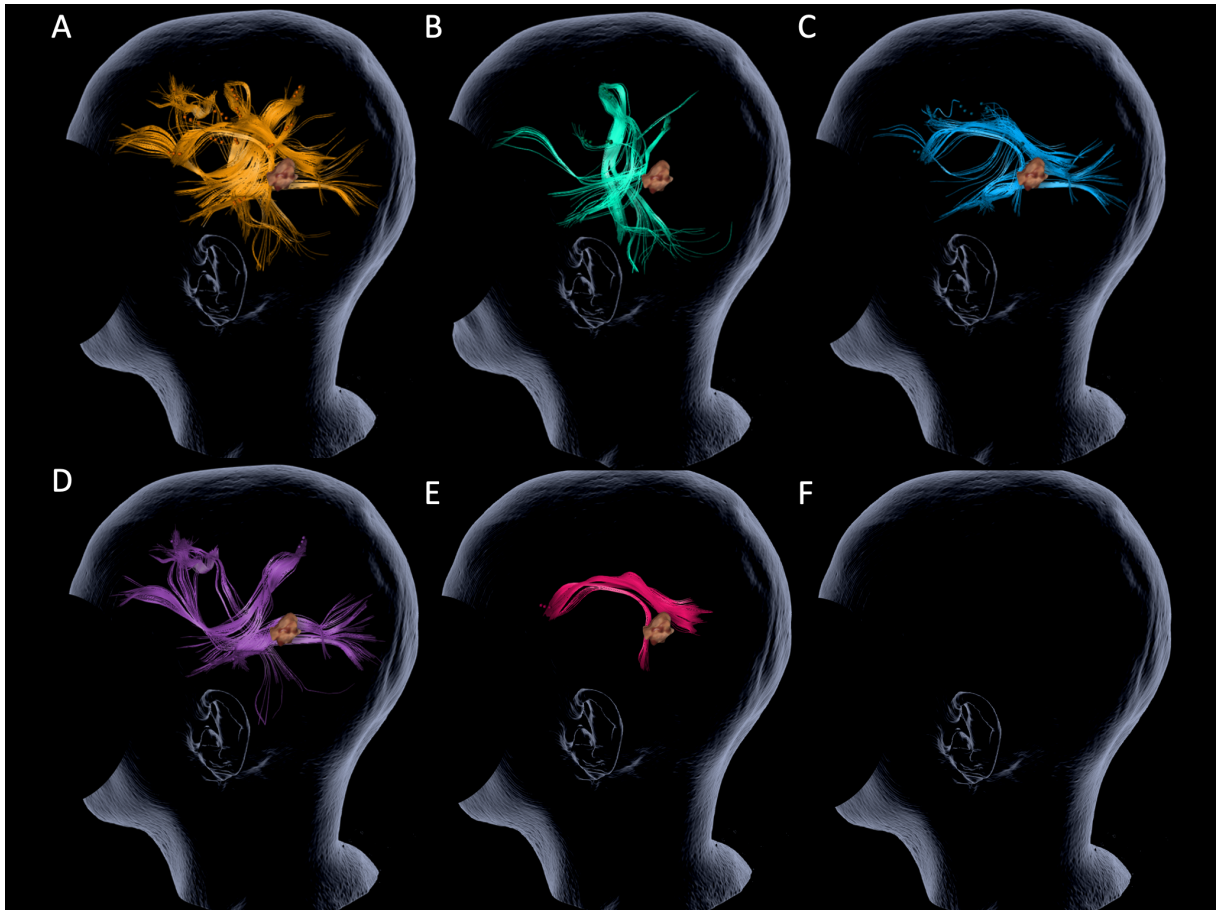


Figure 10.1. Tracked fibers based on the seeds corresponding to different language errors (FA threshold = 0.15).



Figure 10.2. Figure of all seeds and fibers from the figure 10.A to 10.E.

Figure 10.1.A presents the seed and fibers corresponding to all errors except hesitations (in yellow); Figure 10.1.B presents the seed and fibers corresponding to no response (in emerald); Figure 10.1.C presents the seed and fibers corresponding to performance error (in blue); Figure 10.1.D presents the seed and fibers corresponding to hesitations (in purple); Figure 10.1.E presents the seed and fibers corresponding to semantic paraphasias (in red); Figure 10.1.F the brain outline used as the background for presenting the intracranial tracts. Figure 10.2. This figure is the combination of all seeds and fibers from Figures A to E.

The fiber courses were color-coded depending on the error types and displayed in a stereo-image of the brain (Figure 9 and 10). Tumor regions and the following language-related sub-cortical courses of interest were systematically identified: (Catani and Thiebaut de Schotten, 2008; Kuhnt *et al.*, 2012; Axer *et al.*, 2013; Gierhan, 2013; Negwer *et al.*, 2017a): (1) AF; (2) SLF; (3) ILF; (4) UC; (5) FoF; (6) CF; (7) CNT; (8) CtF; (9) ArF.

In evaluating fiber courses based on each nTMS seed, fiber number under each setup of thresholds was documented for the following statistical analysis.

3.8 Statistics

The GraphPad Prism (version 7.0; GraphPad Software Inc., La Jolla, CA, USA) was used for statistical analyses and figure creation.

The descriptive statistics were applied to the demographic data (age, gender, and tumor entities) of enrolled patients, including mean \pm standard deviation (SD), median, minimum, and maximum values. The absolute and relative frequencies of the nine different fiber courses visualized were calculated for each tractography.

The setup of FT thresholds leading to the highest fraction of overall fiber courses visualized among all patients was recorded. Under this threshold, the proportions of patients presenting different tracts considering all errors except hesitations were respectively compared against that of the tractography based on different language errors by X^2 -tests, including no responses, performance errors, hesitations, and semantic paraphasias.

The average ratio (α) of all visualized tracts visualized under each setup of tractography thresholds was used to measure the traceability for each language error category, as follow:

$$\alpha = \frac{R_{AF} + R_{SLF} + R_{ILF} + R_{UF} + R_{FOF} + R_{CtF} + R_{CNT} + R_{CF} + R_{ArF}}{9}$$

In the formula, R represents the proportion of one certain visualized fiber course. 9 is the total number of 9 tracts of interest in the current study. The subscripts describe the 9 tracts, including AF, SLF, ILF, UF, FoF, CtF, CNT, ArF, and CF.

To measure the difference of proportions of visualized fibers between dorsal and ventral pathways among the category of all error without hesitations and the other four categories of linguistic errors, the average ratio (ϵ) of visualized tracts is calculated for the dorsal stream consisting of SLF and AF, while the average ratio (φ) of visualized tracts is calculated for ventral stream consisting of ILF, UF, and AF, as follow:

$$\epsilon = \frac{R_{AF} + R_{SLF}}{2}$$

$$\varphi = \frac{R_{ILF} + R_{UF} + R_{FOF}}{3}$$

Furthermore, a fibers-per-tract Ratio ($\text{Ratio}_{\text{fibers-per-tract}}$) was introduced in the current study, which was defined as the fiber number of visualized fibers ($N_{\text{visualized fibers}}$) divided by the number of visualized tracts ($N_{\text{tracts}} = 9$), as follows:

$$\text{Ratio}_{\text{fibers-per-tract}} = \frac{N_{\text{visualised fibers}}}{N_{\text{tracts}}}$$

This was performed regarding different seeds in each nTMS-based DTI-FT. The Shapiro-Wilk normality test was conducted and indicated the non-normal distribution of the above indexes. These ratios derived from tractography of all errors except hesitations were compared against that of tractography respectively of no responses, performance errors, hesitations, and semantic paraphasias by using Wilcoxon matched-pairs signed-rank tests.

For all statistical comparisons, a p-value under 0.05 was considered statistically significant.

4. RESULTS

4.1 Clinical and Demographic Data

The preoperative nTMS language mapping and nTMS-based DTI-FT were successfully conducted in 40 enrolled patients with different eloquent tumors.

The general demographic information from all enrolled patients is presented in table 1.

Table 1. Demographics of the study cohort

No.	Date of mapping	Gender	Age (Years)	Handess	Pathology	Tumor volume (cm ³)	WHO Grading
1	2016/9/12	m	37.8	L	Ganglioglioma	4.67	1
2	2017/10/24	m	52.0	L	Glioblastoma	28.10	4
3	2017/12/12	f	48.7	R	Anaplastic Astrocytoma	0.44	3
4	2017/9/6	m	76.7	R	Glioblastoma	4.57	4
5	2016/12/9	m	61.7	R	Metastasis	32.50	/
6	2017/4/6	m	68.5	R	Glioblastoma	52.10	4
7	2016/11/17	f	25.9	B	Arteriovenous Malformation	3.08	/
8	2017/3/29	f	33.9	R	Cavernoma	2.07	/
9	2017/10/9	f	47.5	R	Metastasis	13.90	/
10	2017/10/9	m	54.2	R	Glioblastoma	82.70	4
11	2017/9/18	f	47.9	R	Metastasis	0.95	/
12	2017/10/10	m	45.7	R	Oligodendroglioma	13.00	2
13	2016/11/28	m	52.2	R	Glioblastoma	17.80	4
14	2017/11/27	f	70.1	R	Glioblastoma	0.54	4
15	2017/12/27	f	38.6	R	Gangliocytoma	7.20	1
16	2017/12/20	m	64.3	R	Glioblastoma	93.30	4
17	2017/8/28	m	60.6	R	Metastasis	2.40	/
18	2017/8/16	m	72.6	R	Glioblastoma	3.89	4
19	2017/7/11	f	49.9	R	Glioblastoma	5.27	4
20	2017/11/28	m	57.3	R	Glioblastoma	4.12	4
21	2017/11/14	m	71.5	B	Glioblastoma	13.00	4
22	2017/8/2	m	53.4	R	Arteriovenous Malformation	3.20	/
23	2017/8/17	m	55.6	R	Glioblastoma	40.80	4
24	2016/8/18	f	72.2	B	Glioblastoma	5.73	4
25	2016/10/4	f	30.5	R	Pilocytic Astrocytoma	0.32	1
26	2017/5/4	m	66.6	R	Metastasis	2.50	/
27	2017/7/26	f	38.2	R	Pilocytic Astrocytoma	1.44	1
28	2017/8/7	m	74.4	R	Glioblastoma	18.80	4
29	2017/6/26	m	62.0	L	Glioblastoma	39.40	4

30	2017/8/14	m	38.2	R	Metastasis	5.74	/
31	2016/8/24	f	55.1	R	Glioblastoma	61.00	4
32	2018/1/9	f	60.5	R	Glioblastoma	14.90	4
33	2017/5/3	m	42.0	R	Arteriovenous Malformation	1.91	/
34	2018/1/9	m	18.9	L	Pilocytic Astrocytoma	5.83	1
35	2016/10/28	m	59.9	R	Metastasis	41.80	/
36	2017/3/23	m	20.3	R	Glioblastoma	70.20	4
37	2017/12/8	f	80.8	R	Glioblastoma	1.30	4
38	2018/2/8	m	70.6	L	Glioblastoma	24.40	4
39	2018/2/9	f	73.9	R	Metastasis	23.30	/
40	2018/2/19	m	40.6	R	Cavernoma	0.04	/

Table 1. This table presents the general demographic information of the enrolled patients, including mapping date, gender, age, pathological diagnose, WHO grade, and tumor volume.

Before the operation, our team combined these nTMS-based DTI-FT results with clinical examinations for a comprehensive analysis to plan the surgery. According to the feedback from our neurosurgeons, the incorporation of the data derived from nTMS language mapping and nTMS-based DTI-FT was considered helpful in not only planning the resection of the tumor but also suggesting the potentially functional regions for the intraoperative DES during the operation in all cases.

In Table 2, the clinical related characteristics of the cohort are presented. The mean tumor volume was $18.7 \pm 24.1 \text{ cm}^3$ (from 0.1 cm^3 to 93.3 cm^3).

Table 2. Demographic characteristics of patients

Items		Quantity
Number of patients		40
Age (years; mean \pm SD, range)		53.80 \pm 16.00 (18.90–80.80)
Gender (%)	Male	62.50
	Female	37.50
Tumor entities (%)	Glioma WHO grade I	12.50
	Glioma WHO grade II	2.50
	Glioma WHO grade III	2.50
	Glioma WHO grade IV	50.00
	Metastasis	20.00
	Cavernoma	5.00
	AVM	7.50

Table 2 shows the descriptive statistics of patients' demographic information, including the number of enrolled patients, age, gender, and histopathological report of tumor after operations. AVM: arteriovenous malformation; WHO: World Health Organization

Table 3 summarizes the patients' clinical courses at different phases (preoperation, postoperation, and follow-up phase), including the language performance estimations, motor function tests, and Karnofsky Performance Status (KPS) scores. Assessment of the language status was classified into four grades (from grade 0 to 3). The British Medical Research Council (BMRC) scale of muscle strengths was used to estimate the motor function in every patient and then classified into two categories, BMRC = 5/5 representing the motor integrity and BMRC < 5/5 indicating motor deficits in different levels. The median and range of KPS were also calculated.

Table 3. Summary of clinical data

Function categories		Grades	Percentage
Language function	preoperative status (% of patients)	Grad 0	62.50
		Grad 1	17.50
		Grad 2	17.50
		≥Grad 3	2.50
	postoperative status (% of patients)	Grad 0	50.00
		Grad 1	25.00
		Grad 2	20.00
		≥Grad 3	5.00
	Clinic follow-up (% of patients)	Grad 0	65.00
		Grad 1	20.00
		Grad 2	10.00
		≥Grad 3	5.00
	Surgery-related deficits (% of patients)	None	77.50
		Transient	10.00
		Permanent	12.50
	Motor function	preoperative status (% of patients)	BMRC = 5/5
BMRC < 5/5			7.50
postoperative status (% of patients)		BMRC = 5/5	80.00
		BMRC < 5/5	20.00
Clinic follow-up (% of patients)		BMRC = 5/5	92.50
		BMRC < 5/5	7.50
Surgery-related deficits (% of patients)		None	85.00
		Transient	12.50
		Permanent	2.50
KPS scores		preoperative status (% of patients)	Median
	Range		50.00~100.00
	postoperative status (% of patients)	Median	80.00
		Range	50.00~100.00
	Clinic follow-up (% of patients)	Median	90.00
		Range	40.00~100.00

Table 3 provides detailed descriptive statistics of the clinical examination on the patients, including values for aphasia level, muscle strengths, and Karnofsky Performance Status (KPS) scores.

Friedman-tests on the clinical aphasia scores from the preoperational, postoperational, and follow-up phases showed a significant difference among the three conditions (Figure 11). The level of postoperational aphasia increased significantly compared to the aphasia levels in both preoperational and follow-up phases. However, there was no significant difference in aphasia levels between the preoperational and follow-up phases (Figure 11).

Correlation analysis showed that the pathological diagnoses were correlated to the preoperative aphasia scores ($r = 0.392$, $p = 0.012$) but not to the postoperational aphasia scores ($r = 0.039$, $p = 0.810 > 0.05$), nor to the follow-up scores ($r = 0.042$, $p = 0.797 > 0.05$).

Friedman test of aphasia scores among preoperation, postoperation and follow-up

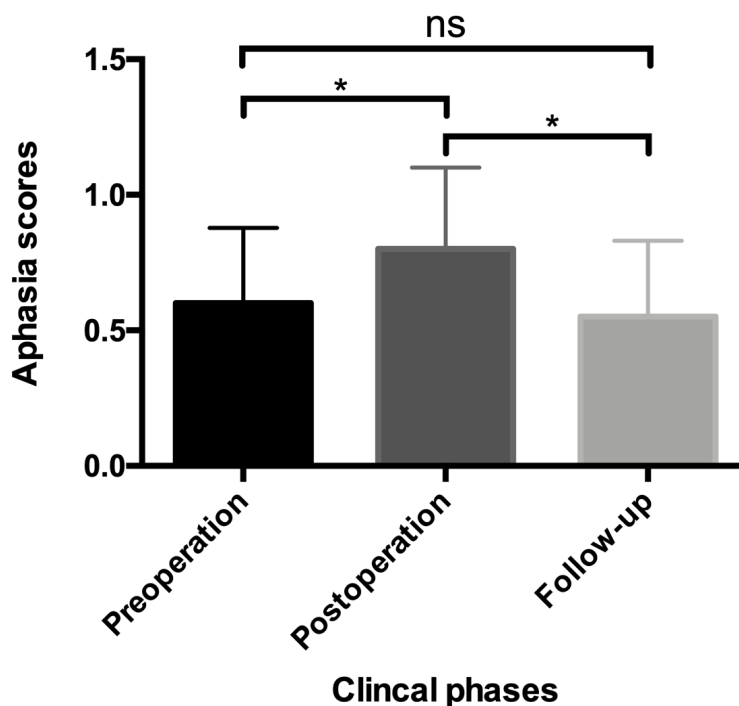


Figure 11. Comparison of aphasia scores among the preoperational phase, postoperational phase, and follow-up phases.

Figure 11. In this figure, the result of the Friedmann nonparametric analysis showed significant differences among the aphasia levels in the preoperational, postoperational, and follow-up phases (ns: no significant difference; *: $p < 0.05$)

Considering tumors located in the language-eloquent areas, the proportions of patients with grade 1 and 2 aphasia increased respectively from 17.50% to 25.00% and from 17.50% to

20.00% after the operation. During the follow-up phase, the proportions of patients with grade 1 and 2 aphasia decreased to 20.00% and 10.00%, respectively. It is noted that the proportion of patients without aphasia in the follow-up phase (65.0%) increased by 2.50% compared with the preoperative phase (62.50%). When comparing preoperative and postoperative language functions, 10.00% of patients suffered from transient surgery-related aphasia, and 12.50% were diagnosed with permanent surgery-related language deficits at different levels. The 77.50% of patients who did not experience a decrease in language function and the patients with the transient language deficit (10.00%), hence, resulted in 87.50% of patients preserving their intact language function after surgery.

Regarding changes in muscle strength, 20.0% of patients had a decreased muscle strength after surgery. However, during follow-up, the proportion of patients with muscle weakness was the same as that in the preoperational phase.

The KPS Median decreased by 10.0% after surgery. However, during the follow-up, though the expanded range of scores was found during follow-up, the median KPS score went back to the preoperative level.

Preoperative sensory deficits were recorded in 7.50% of patients in other clinical physical examinations, whereas patients with sensory deficits after surgery increased by 2.50% during follow-up examinations. According to their medical records, 45.00% of patients had experienced epileptic seizures preoperatively, whereas only 25.00% suffered from seizures during the follow-up phase. Regarding the antiepileptic drugs, 86.30% of patients took levetiracetam, 6.90% took prescribes of levetiracetam and valproate, 3.40% were treated with levetiracetam and carbamazepine, and 3.40% were treated with levetiracetam and phenytoin.

4.2 Mapping and Tractography

Regarding the simulation setup, the ipsilateral rMT measurements in the left hemisphere were successfully conducted in all subjects with an average rMT of 36.75 ± 8.80 , ranging from 21.00 to 59.00. While contralateral rMT measurements were performed in 35 patients, resulting in an rMT of 37.97 ± 9.09 with a range of 22.00~60.00. There was no significant difference between the hemispheres according to paired t-tests.

There were 39 patients presenting more than one naming error. Regarding the different categories of naming errors, 36 patients (90.00%) presented no-response errors, 35 patients (87.50%) presented performance errors, 16 patients (40.00%) presented hesitation, and semantic paraphasias were found in 30 patients (75.00%).

The traceability of language-related fibers at different adjustments was evaluated in each of the five error categories. The CNT has displayed the highest ratio of traceability among all fibers under every adjustment, which was followed by the CtF except under the adjustment of 100% FAT (Table 4).

The 100% FAT from different types of naming errors was recorded. The 100% FAT corresponding to all errors except hesitations is 0.33 ± 0.08 , at the range of 0.20 ~ 0.51. In the category of no response, its 100% FAT is 0.31 ± 0.07 , ranging from 0.19 to 0.47. The 100% FAT of performance errors is 0.29 ± 0.07 , ranging from 0.17 to 0.46. The 100% FAT

corresponding to the hesitation and semantic paraphasias is both at 0.29 ± 0.07 , but their ranges are different. The 100% FAT ranges from 0.19 to 0.40 in the category of hesitation, while in the category, it is 0.29 ± 0.07 ranges between 0.13 and 0.51.

The 100% FAT from different types of naming errors were compared using ANOVA, followed by the Bonferroni test to correct for multiple comparisons, from which no significant differences were found (Figure 12).

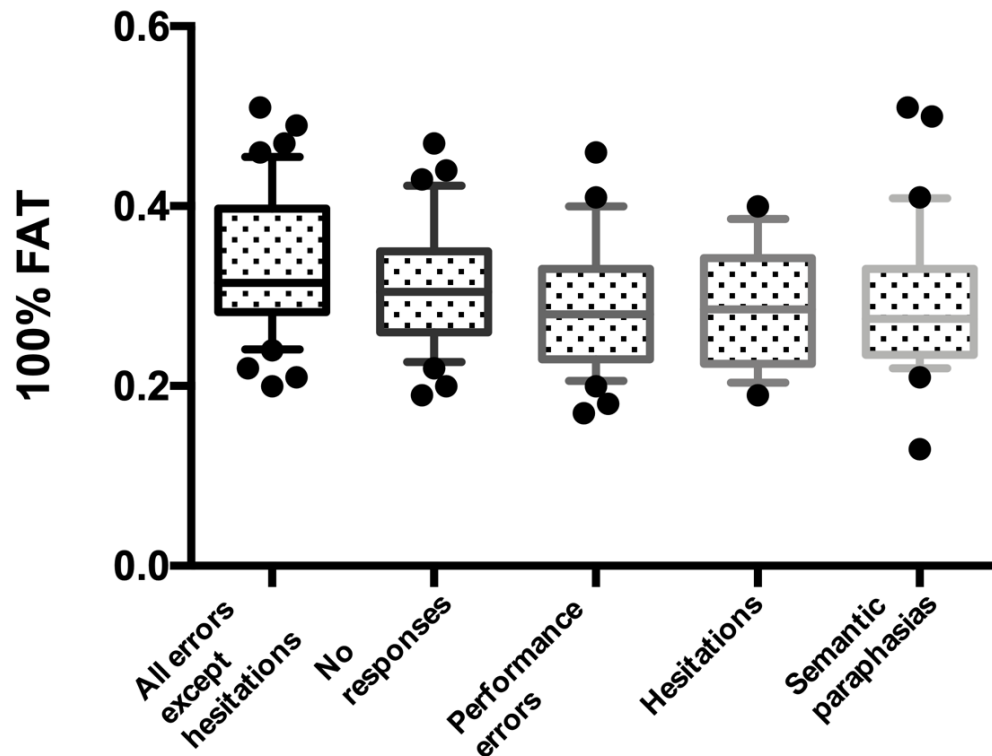


Figure 12. ANOVA of 100% FAT among different types of naming errors with Bonferroni corrections for multiple comparison.

Figure 12. As shown in the figure, there are no significant differences among different types of naming errors ($p > 0.05$). The whiskers above and below indicate the 10 ~ 90 percentile of the data.

According to the results, the highest traceability (55.90%) of visualized tracts during nTMS-based DTI-FT in the group analysis was using the threshold of the FA of 0.10 and the FL of 100.00 mm when compared to the traceability under other adjustments (Table 4) ($p < 0.0001$). It suggests that the application of FAT = 0.10 during fiber tracking in the current study can best present subcortical fibers. Thus, results from the analysis with this adjustment were used for the subsequent analysis.

In the following parts, detailed analyses of DTI-FT based on the respective error category in nTMS language mapping are presented.

Table 4. Fractions of visualized tracts among all patients under different tracking adjustments

Tractography setups			Language-related tracts (%)								α
FA	FL(mm)	ArF	CF	AF	CNT	CtF	SLF	ILF	UC	FoF	
0.10	100.00	24.50	69.50	60.50	72.00	68.00	61.00	61.50	25.00	62.00	55.90
0.15	100.00	9.00	58.00	54.00	68.50	57.50	42.00	51.50	11.00	50.00	44.60
100%FAT	100.00	1.00	6.50	18.50	40.00	3.00	7.00	11.00	1.00	18.00	11.80
75%FAT	100.00	5.00	37.00	34.00	62.00	40.50	18.50	30.00	1.50	37.00	28.40
50%FAT	100.00	7.50	58.00	52.50	71.50	64.00	42.00	52.00	12.00	53.50	45.90

This table shows the percentage of visualized tracts resulting from the analysis on the tractography under different setups consisting of FA (FA = 0.10, 0.15, 100% FAT, 75% FAT, and 50% FAT) and FL (100.00mm). The fractions are presented for AF, SLF, ILF, UC, FoF, CF, CNT, CtF, and ArF. α indicates the average ratio of visualized tracts in each category of tractography setups. The traceability under FA = 0.10 is at the highest ratio compared with other setups ($p < 0.0001$).

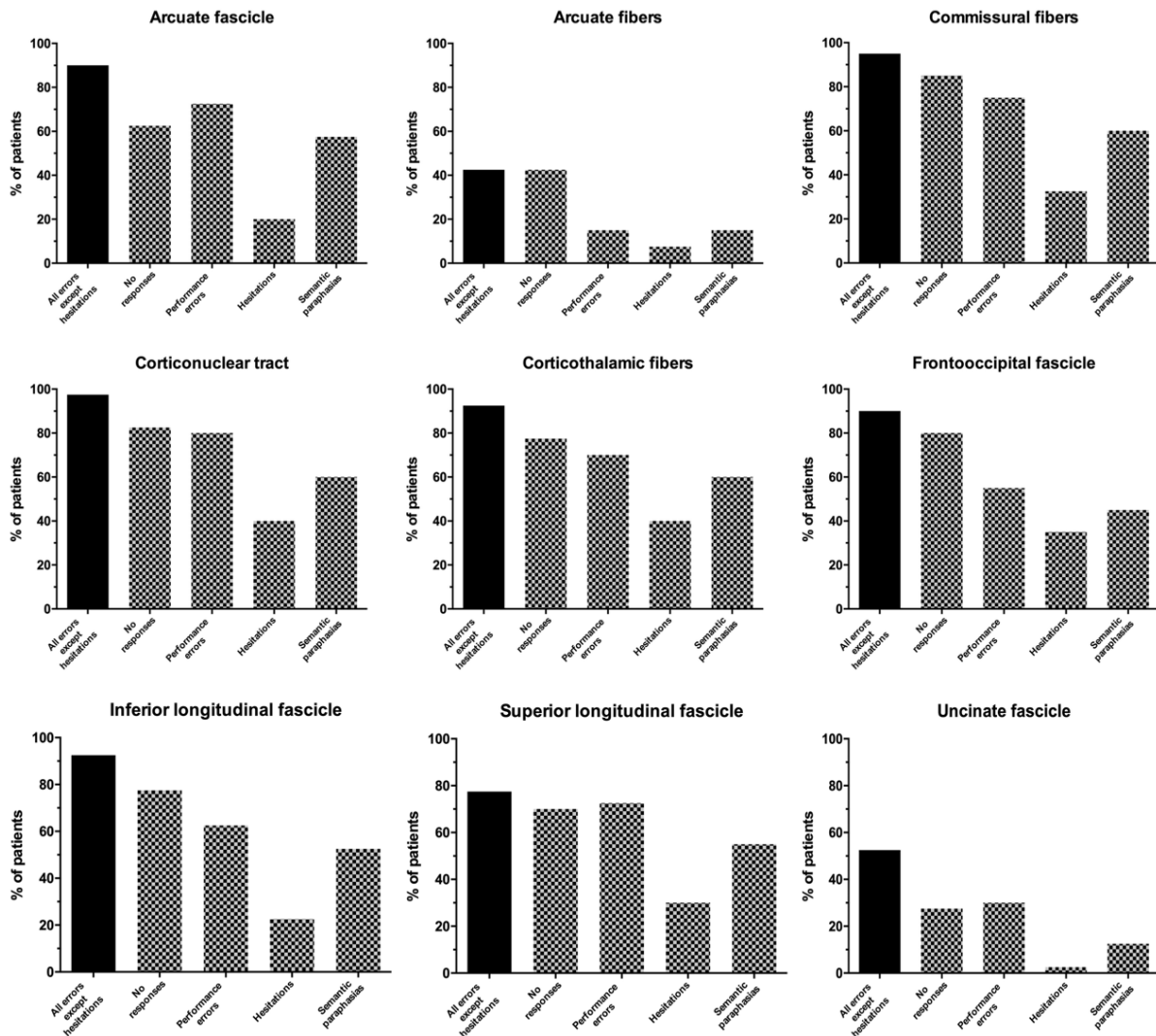


Figure 13. Percentage of each neual tract corresponding to different naming errors

Figure 13. The figure shows the percentage of patients presenting 9 tracts of interest corresponding to each error type. Each subfigure corresponds to a respective tract.

4.3 Ratios of Patients Presenting Visualized Fibers

The best traceability was detected with FA = 0.10, under which the ratio of patients presenting visualized fibers was calculated.

All errors except hesitations were considered the most commonly used category in nTMS-based DTI-FT for subcortical language-related tracts. In the current study, its tractography of the corresponding seeds resulted in the high fractions of visualized tracts, 81.10% of patients presenting at least one of the above tracts during analyses (Figure 13). Regarding the category of no responses, 67.20% of patients presented more than 1 neural tract in tractography. The category of performance errors comes the second, in which 59.20% of patients showed the tracts mentioned above (Figure 13). Followed by the category of semantic paraphasias, in which 46.40% of patients presented different tracts. In the end, it's the category of hesitations; only 25.60% of patients presented the various tracts according to their results from nTMS-based DTI-FT (Figure 13).

4.4 Numbers of Fibers and Ratio_{fibers-per-tract} in Tractography

When using the seeds from the category of all errors except hesitations for tractography, the total number of the tracked fibers is 3896.10 ± 2437.60 (ranging from 731.00 to 10468.00) displayed in figure 14, resulting in a Ratio_{fibers-per-tract} is at 538.40 ± 340.50 (range 119.80 ~ 1416.30).

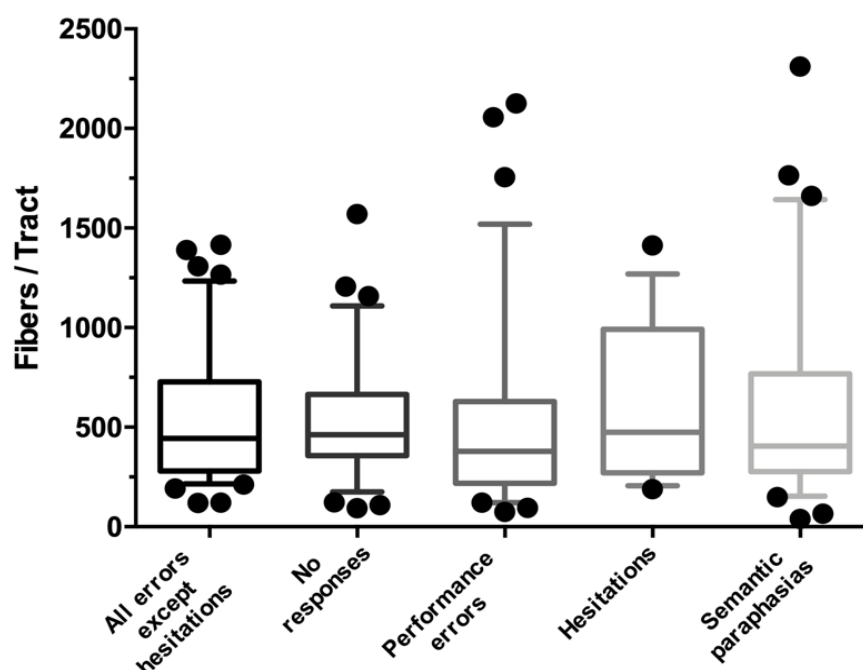


Figure 14. Comparison of the ratio of fibers/tracts among different categories of naming errors.

Figure 14. This figure presents the ratio of fibers/tracts based on 5 categories of naming errors, including all errors except hesitations, no response, performance errors, hesitation, and semantic paraphasias. The whiskers above and below indicate the 10 ~ 90 percentile of data.

The fiber number resulting from tractography in the no response category is 3618.70 ± 2171.80 (ranging from 649.00 to 9648.00) detected in total. Furthermore, the $\text{Ratio}_{\text{fibers-per-tract}}$ corresponding to the no response category is 548.60 ± 325.80 (ranging from 92.70 to 1570.00) (Figure 14). The $\text{Ratio}_{\text{fibers-per-tract}}$ of nTMS-based DTI-FT from seeds corresponding to the category of all errors except hesitations and the $\text{Ratio}_{\text{fibers-per-tract}}$ from the category of no responses were compared, resulting in no statistical significance ($p = 0.4507$).

The total number of fibers visualized in nTMS-based DTI-FT from seeds of performance errors is 3107.10 ± 2680.70 (ranging from 189.0 to 12288.0). Then, the $\text{Ratio}_{\text{fibers-per-tract}}$ is calculated, resulting in 545.30 ± 519.70 (range: 74.2 – 2125.2) (Figure 14). However, there was no statistical significance between tractography based on the seeds of all errors except hesitations and seeds of performance errors ($p = 0.5223$).

Regarding the category of hesitation, the tractography based on its seeds resulted in the number of tracked fibers was 3447.00 ± 2239.90 (range: 1068.00 – 9891.00), then its $\text{Ratio}_{\text{fibers-per-tract}}$ was 632.60 ± 394.70 with a range from 188.70 to 1413.00 (Figure 14). No significant differences of $\text{Ratio}_{\text{fibers-per-tract}}$ are detected in the comparison between the category of all errors except hesitations and the category of hesitations ($p = 0.2312$).

In the tractography for semantic paraphasias, the total number of tracked fiber was 3282.00 ± 2762.40 (range 240.00 – 11556.00). The $\text{Ratio}_{\text{fibers-per-tract}}$ was 605.90 ± 533.20 (range 40.00 – 2311.20) (Figure 14). No significant difference was detected between $\text{Ratio}_{\text{fibers-per-tract}}$ from the category of all errors except hesitations and $\text{Ratio}_{\text{fibers-per-tract}}$ from the category of semantic paraphasias ($p = 0.5425$).

4.5 Analysis of Ventral and Dorsal Streams

The ratio of visualizing the two streams corresponding to different categories was calculated, respectively (Table 5).

Table 5. Analysis of ventral and dorsal streams

Category	The (ϵ) ratio of visualizing the ventral stream (%)	P (1) value	The (φ) ratio of visualizing the dorsal stream (%)	P (2) value
All errors except hesitations	62.50		60.00	
No responses	49.17	0.04	56.25	0.63
Performance errors	35.83	<0.01	47.50	<0.01
Hesitation	10.83	<0.01	18.75	<0.01
Semantic paraphasias	26.67	<0.01	35.00	<0.01

Table 5. P (1) value: The K-square test between the ratio of the ventral stream from the category of all errors except hesitations and that from the other 4 categories (no responses, performance errors, hesitations, and semantic paraphasias).

P (2) value: The K-square test between the ratio of the dorsal stream from the category of all errors except hesitations and that from the other 4 categories (no responses, performance errors, hesitations, and semantic paraphasias).

The ratio of the ventral stream from the category of all errors except hesitations is higher than that from the other 4 categories (Table 5). And the ratio of the dorsal stream from the category of all errors except hesitations is higher than that from the categories consisting of performance errors, hesitation, and semantic paraphasias, except the category of no responses (Table 5).

5. DISCUSSION

This study focused on the visualization of language function-related neural tracts in patients with tumors in language-eloquent regions. With nTMS applied in the preoperative phase for the language mapping, the language-related cortex was identified and later used as the seed regions for the fiber tracking. The optimal adjustment resulting in the best visualization of neural tracts was determined by comparing different parameters used for tractography. Then, this adjustment was applied in the setup for the comprehensive analysis on the nine different subcortical tracts of interest, which were known to be language-related from previous pieces of literature.

The analysis of nTMS-based DTI-FT was founded on the different types of naming errors, namely all errors except hesitations, no responses, performance errors, hesitations, and semantic paraphasias. The dorsal and ventral streams were demonstrated to be related to all kinds of naming errors, suggesting their hierarchical or multi-layered functional collaboration for processing linguistic information.

5.1 nTMS and the Prognosis of Language Function

The previous studies demonstrated that the pathological diagnosis of the intracranial lesion is correlated to the postoperative survival time (Porter *et al.*, 2011; Liang *et al.*, 2020); however, its relationship with the language function has not been systematically investigated. The current study showed that the pathological diagnoses were only correlated with the preoperational aphasia states ($r = 0.392$, $p = 0.012$), while it is not correlated with the aphasia scores in the other phases (postoperation: $r = 0.039$, $p = 0.810 > 0.05$; follow up: $r = 0.042$, $p = 0.797 > 0.05$). Pathological investigation can indicate not only the growth rate and malignancy of the tumor cells but also the genetic mutations, for example, IDH, P53. Those pathological changes are closely related to the severity of the brain lesions (Rees, 2011); however, the postoperative functional recovery levels are currently considered to be related to brain plasticity (Duffau *et al.*, 2003), which may lead to that the functional postoperative prognosis is not correlated with the pathological diagnosis.

Surgery-related transient aphasia occurs in 10% of patients enrolled in this study; meanwhile, permanent aphasia associated with surgery occurred in 12.50% of patients. The permanent aphasia patients increased by 2.50%, while the patients with grade 2 aphasia decreased to 10% from preoperative 17.5%, and the patients with grade 0 or grade 1 aphasia increased by 5.00%. Regarding the difference in the language function between the follow-up and preoperative phase, 12.50% of the patients got worse function, whereas 17.50% of the patients showed significant improvement in language function at the follow-up phase. Among the patients manifesting a permanent functional decline, only one patient was diagnosed with grade 3 aphasia during follow-up.

Outcomes in our study were consistent with previous reports using DES. In previous articles, they measured the short-term and long-term prognosis of linguistic functions in patients

receiving DES during the glioma resection, which demonstrated the probability of transient aphasia appearing postoperatively ranges from 14.00 % to 50.00 % (Sanai *et al.*, 2008; Duffau *et al.*, 2009b; Wilson *et al.*, 2015; McCarron *et al.*, 2017), while the permanent functional deterioration occurs in 5.00 % to 20.00 % of the cases (Sawaya *et al.*, 1998; Taylor and Bernstein, 1999; Brell *et al.*, 2000; Chang *et al.*, 2003). Given that the entire group of patients presented with tumors in left-hemispheric, language-eloquent regions, the nTMS combined with DTI-FT showed that the tumor did not totally invade the cortical and subcortical language-related regions. Combining the results of nTMS mapping to formulate a reasonable surgical plan makes the total resection of intracranial tumors being conducted more safely and better avoid surgery-related damage to language-related brain structures. Only 5% of the patients in this study developed grade 3 aphasia after surgery, which supported that the combination of nTMS and DTI-FT for preoperative functional localization helps improve the patients' prognosis.

Therefore, the current study suggested that the combination of preoperative nTMS language mapping and nTMS-based DTI-FT can not only provide guidance for planning the surgery but also potentially benefit the functional prognosis. However, a randomized controlled trial regarding this relation is needed in the future.

5.2 nTMS-based DTI-FT for Language Function

It is demonstrated in the previous study that the tractography based on the nTMS mapping results can support the preoperational visualization of subcortical structures (Raffa *et al.*, 2016). In Raffa's study, they defined different approaches to set seeds for the subsequent tractography analysis, consisting of (1) seed of all language-positive nTMS spots (all-spots strategy), (2) seed of each single language-positive nTMS spot for FT respectively (single-spot strategy), and (3) using anatomical ROI seeding (standard FT strategy) (Raffa *et al.*, 2016). The tractography results, respectively, based on those three seeds used for visualizing the complex cortico-subcortical language network were accessed and compared (Raffa *et al.*, 2016). Their comparisons showed that the nTMS-based DTI-FT is superior to the other FT approaches by better presenting the cortical and subcortical neural connections related to the language functions.

The above-mentioned point established the important theoretical bases of the methods used in the current study. However, the differences compared to our approach are needed to be noticed:

- (1) "single-spot" strategy (Raffa *et al.*, 2016) was not used in the current study. We only defined the cortical seeds according to the naming errors. Tractography in the current study was purely based on nTMS language mapping, neither defining the anatomical seed nor counting the number of spots connected. Seeds related to one type of naming errors were combined for the DTI-FT to generate a better view of the language-related network;
- (2) Only a small cohort has been used in Raffa's study (Raffa *et al.*, 2016). We expanded the sample size to 40 cases to increase the stability and reliability of the research results. At the same time, the tracts of interest were expended to 9, to achieve a more

detailed picture of the subcortical network;

- (3) We introduced a new category, "all errors except hesitation," in the seeding process and used it as a control group in comparisons to analyze the differences among various aspects of the language;
- (4) The dependency of tract visualization on ROIs consisting of different error types as evaluated in the current study has not been systematically explored in the past. It should be noticed that the different aspects of cerebral functions are involved in different naming errors. The exploration of language functions based on different naming errors respectively, rather than combined as a single category, can present the different aspects of linguistic function. Results of the current study and the previous one by Raffa *et al.* should not be compared directly. In Raffa's study, their interpretation was only partially consistent with ours regarding the associations between error types and subcortical tracts.
- (5) Based on previous literature, the current study introduced the "dual-stream" model to define the role of the streams concerning naming errors. Different fibers are regarded as a functional unit in analysis (Buchsbaum *et al.*, 2005; Axer *et al.*, 2013; Fridriksson *et al.*, 2016; Dittinger *et al.*, 2018), which is consistent with the current view widely recognized in the domain of neuroscience: the generation and output of brain function are the results of the synergy between different networks and neural tracts (Fornito *et al.*, 2012).

5.3 Language-related Tracts

The nine different subcortical language-related pathways related to language are investigated and focused on in the current study, consisting of AF (Rolheiser *et al.*, 2011), SLF (Kamali *et al.*, 2014), ILF (Steinbrink *et al.*, 2008; Lebel *et al.*, 2013), UF (Friederici and Gierhan, 2013), FoF (Ille *et al.*, 2018), CF (Negwer *et al.*, 2017a; Negwer *et al.*, 2017b), CNT (Love and Webb, 2008), CtF (Crosson, 2013; Negwer *et al.*, 2017a), and ArF (Bhatnagar, 2018). Our results supported the emerging conceptualization of the language processing system posits that the integrity of white matter tracts reinforces different aspects of information processing (Sollmann *et al.*, 2015a; Sollmann *et al.*, 2016b; Negwer *et al.*, 2017b; Ille *et al.*, 2018; Negwer *et al.*, 2018).

According to previous studies, the AF is considered the major subcortical fascicle in maintaining language processing, and its damages are related to different kinds of aphasia (Leclercq *et al.*, 2010; Maldonado *et al.*, 2011). Moreover, phonological errors can be seen when the AF is stimulated using intraoperative DES (Duffau *et al.*, 2002; Leclercq *et al.*, 2010; Maldonado *et al.*, 2011; Chang *et al.*, 2015). Phonological errors are not commonly detected in nTMS language mapping; hence they were not included in the current study (Lioumis *et al.*, 2012b; Picht *et al.*, 2013; Krieg *et al.*, 2016). Additionally, AF's microstructure was found related to the development of literacy skills (Broce *et al.*, 2019). Regarding the different error types, AF was most frequently visualized in semantic paraphasias and hesitations (Raffa *et al.*, 2016); however, in the current study, the AF was mostly observed through performance errors (72.50%) and semantic paraphasias (57.50%) compared to other naming errors. Although both Raffa's

study and ours were performed in Germany and only enrolled German native speakers (Raffa *et al.*, 2016), bilingualism was not taken into consideration in either of the studies, which could lead to different results on AF. It has been demonstrated that long-term training experience in bilingual circumstances can lead to more structural connections in the left AF when compared with monolinguals (Hamalainen *et al.*, 2017).

The injured SLF has shown to be predominantly correlated to speech arrests, dysarthria, and other articulatory impairments in previous studies (Leclercq *et al.*, 2010; Galantucci *et al.*, 2011; Broce *et al.*, 2019). In the current study, it was observed that the ratio of SLF visualization was comparatively high in different error categories: performance errors (72.50%), no responses (70.00%), and semantic paraphasias (55.00%) (shown in figure 14). Both the AF and SLF are regarded as major fiber tracts in the dorsal stream, involving language-related motor processes (Chang *et al.*, 2015). Therefore, nTMS on the AF and SLF inducing a high fraction of performance errors supported the role of the dorsal stream in language function (Krieg *et al.*, 2016).

Most studies just considered the ILF as a part of the ventral stream, then merged its analysis with the FoF, thus impeding the clear interpretation of its associations with specific language functions and/or error types (Mandonnet *et al.*, 2007). Currently, the ILF was mostly suggested to be related to the maintenance of semantic processing (McKinnon *et al.*, 2018). Additionally, Raffa indicated that the most frequent error type among connected regions by the ILF was semantic paraphasias (Raffa *et al.*, 2016). This is also supported by Herbet's findings that confirmed the ILF playing a role in lexical retrieval in healthy brains (Herbet *et al.*, 2018). In the current study, the ILF was not the most visualized tract for semantic paraphasias, but it was visualized in most patients with semantic paraphasias (60.00%). We considered reasons behind this might be that semantic paraphasias are rarely observed during nTMS language mapping, thus hampering in interpreting the nTMS-based DTI-FT for this category. This problem was also mentioned in previous studies (Sollmann *et al.*, 2015d; Raffa *et al.*, 2016). More techniques should be considered for a hybrid analysis to compensate for the rare occurrence of semantic paraphasias.

The FoF was considered a neural tract associated with semantic language processing and goal-oriented behavior (Conner *et al.*, 2018). However, semantic paraphasias are hardly induced during nTMS language mapping, hindering the application of nTMS-based DTI-FT for this error type (Figure 14). In the current study, the FoF was detected in 80.00% of cases under the no response category, while only in 45.00% employing the category of semantic paraphasias. Although not fully delineated until now, the FoF was related to language functions, such as reading and writing (Fekonja *et al.*, 2019). The role of the FoF in language still needs further study.

The CF was detected in 87.50% of patients presenting no response and 80.00% of patients presenting performance errors, which supported the view that CF was a crucial fascicle for the speech-language functions (Witruk *et al.*, 2002; Love and Webb, 2008). It is evident from a case study that the posterior CF is a vital structure in communicating information between the occipital cortex in the right hemisphere and the language centers in the left hemisphere (Mulroy *et al.*, 2011).

CtF was engaged in language-related neural networks to support the language function (Crosson, 2013). Previous studies demonstrated that the thalamus was not directly involved in

linguistic processing but rather as a central monitor or a hot hub for connecting language-related cortices. The basal ganglion might participate in linguistic perception and production (Crosson, 2013; Klostermann *et al.*, 2013). In the current study, the CtF was found in 77.50% of cases under the no response category, 70.00% with performance errors, and 60.00% with semantic paraphasias. This underlines that the CtF has a multi-level role in language.

The CNT was found in 82.50% of patients with no response and 80.00% of the performance errors in the current study. No response errors indicate a certain degree of movement disruption, including mouth and tongue movements. The CNT seems crucial in the facial and oral movement (Halpern, 1986), meanwhile, takes part in linguistic plasticity (Northam *et al.*, 2019).

There are different views on the involvement of UF in language production. Duffau *et al.* reported that the stimulation on UF was not able to induce language disorders during Neurosurgery (Duffau *et al.*, 2009a). In 2011, Galantucci also indicated that the impairment of UF was not associated with the aphasia levels (Galantucci *et al.*, 2011). But, in the same year, Papagno *et al.* recorded the obvious naming deficits in patients immediately after the tumor resection of LGG located in UF and also in the 3 months follow-up (Papagno, 2011; Papagno *et al.*, 2011), including the object recognition, reduced verbal fluency, and anomia (Papagno *et al.*, 2011). In the current study, the UF was visualized only in 12.50% of patients presenting semantic paraphasias. The differences in the conclusions on the UF and its relationship with language were observed from different studies. In the current study, the UF was detected in 30.00% of patients with performance errors and 27.50% of patients with no response. This ratio is smaller than other intracranial tracts, and it presents the involvement of UF in language processing at a lower level. There are several potential reasons for this phenomenon, for example, 1) different studies enrolled subjects with different mother tongues; 2) the variable tumor locations among subjects affected brain functions at different levels, 3) the plasticity of language function will cause differences in the individualized distribution of brain functions.

In the study by Negwer *et al.*, the nTMS-based DTI-FT for language function can increase the visualization of short fibers, such as ArF and UF (Negwer *et al.*, 2017b). The role of ArF in language has not been well elaborated in their article. The current study found that ArF's participation in no response (62.50%) was higher than in other language error categories. The role of short fibers in the language-related subcortical network needs more investigations to clarify its respective functions.

5.4 Different Categories of Naming Errors

In the current study, the no response category was involved with the highest ratio in visualizing the IFL, FoF, CF, CNT, CtF, and ArF. It indicates the involvement of these fibers in processing language, but their respective major functions still cannot be identified. AF is regarded as an important component in language development, enhancing language learning, and monitoring speech (Bernal and Ardila, 2009), which might also contribute to this naming error. The CNT consists of fibers from motor neurons and contains important links to connect different key nucleus and cortices for modulating the output of the attempted speaking motion. From the perspective of motor neurons related to vocalization muscles, it is reasonable for CNTs to be

related to no response fibers. To understand the relationship between other fibers and no response, we still need further research.

Errors of no-response are easier to be identified and defined compared with other categories. In earlier times, the category of no responses was considered the main category during nTMS language mapping by other groups (Pascual-Leone *et al.*, 1991; Epstein *et al.*, 1999). Furthermore, the variability of inter- and intra-observer has been rarely reported in the no-response category (Sollmann *et al.*, 2013). Another study also suggested that this error could be easily distinguished in earlier investigations (Pascual-Leone *et al.*, 1991; Epstein *et al.*, 1999). In terms of nTMS-based DTI-FT, it is possible to achieve comprehensive tractography results when relying on the no-response category alone. Furthermore, the fibers-per-tract ratio of no-response was not significantly different from the category of all errors except hesitations (Figure 14); thus, it demonstrated that they shared a similar tractography.

Regarding the category of hesitations, only 16 patients (40.00%) presented hesitations during the mapping in the current study. When employing the seeds of this category for following DTI-FT, there were not as many visualized tracts of interest as the other categories (Figure 13), though the fibers-per-tract ratio of hesitations is without significant difference with other categories (Figure 14). The percentage of patients presenting the various tracts related to hesitations is not as high as other naming error categories (Figure 13). For an objective measurement of hesitation, the vocal latencies during nTMS should be compared with the corresponding baseline. It should be noticed that our subjects were brain tumor patients in the current study, who tend to experience fatigue and dry mouth more often than healthy people during the language mapping, which will affect the measurement of vocal latency time. As a consequence, the possibility exists that objective hesitation errors probably do not occur during stimulation. So, we need to be conservative about hesitation errors. A method for objectively measuring and testing the latency time for hesitations remains to be further developed.

In prior work, performance errors were interpreted as a disturbance in speech production and perception. In the category of performance error, the CNT was mostly detected (80.00%), and the second most is CtF (77.50%) (Figure 14). It is worth noting that there have been no detailed studies in nerve tracts related to this language error in previous pieces of literature.

Semantic processing carries out the linking of the word forms and their related meaning. Disruption to this connection is seen in the present study in semantic paraphasias, where patients utter a semantically related word instead of the correct target. During object naming tasks, incorrectly performed semantic processing may lead to the substitution of the target word to a semantically similar or associated word. In the current study, besides UF and ArF, other seven tracts of interest can be visualized in more than 40.00% of patients (Figure 13). The semantic processing could be disturbed by the repeated nTMS influencing phonological code retrieval, syllabification, phonetic encoding, and articulation components of the language processing (Indefrey and Levelt, 2004; Strijkers and Costa, 2011; Tate *et al.*, 2014), which were parts of processes needed in naming objects and actions (Krieg *et al.*, 2016). Raffa's study suggests that semantic paraphasias and hesitations were the most frequent error types regarding the AF, while semantic paraphasias were also the most frequent category when considering the ILF and inferior FoF (Raffa *et al.*, 2016). These tracts were also visualized in most patients in the current study during the tractography regarding the category of semantic paraphasias.

However, our results cannot be compared directly with that from Raffa's study because in the current study: 1) the study protocol differed, and no anatomically located seeds were used; 2) more patients were included.

5.5 Ventral/Dorsal Stream & nTMS-based Language-related Tractography

Processes of verbal expression are grounded in a neural architecture that accomplishes the integration of auditory object recognition in combination with sequential prediction, which requires intact structures of ventral/dorsal streams (Bornkessel-Schlesewsky *et al.*, 2015). When comparing each naming error (no response, hesitations, performance errors, and semantic paraphasias) with all errors without hesitations, there were significant differences found in all pairs of comparisons on both the ventral stream and the dorsal stream, except the comparison between the dorsal stream from no response's category and that from all errors without hesitation. This result showed that the dorsal and ventral streams were related to almost all kinds of naming errors.

Firstly, it's worth discussing the functional cooperation of the two streams. In the current study, both streams from single error are much smaller than that from all errors except hesitations, which indicates that they may be jointly involved in linguistic performance at different levels and in the different naming processes. This conclusion underlines that language function is likely to be a synergistic system involving different subcortical tracts rather than a segregated system, which is supported by Rolheiser's study (Rolheiser *et al.*, 2011).

Secondly, the lack of significant difference in the dorsal stream ratio between the category of all errors without hesitations and the category of no response could indicate that the dorsal stream could be dominant in the occurrence of the no response. Referring to the previous studies, the disruption of the motor controlling aspect of vocal organs leading to no response or performance errors was related to the dorsal stream (Loui, 2015). Henry *et al.* showed that phonological performance was impaired in patients with damages to dorsal pathway structures (Henry *et al.*, 2016). The Kummerer *et al.* demonstrated that the individual lesion on the dorsal stream showed a significant correlation with a deficit in linguistic repetition performance, and lesions on tracts related to the ventral stream were associated with deficits in comprehensive performance (Kummerer *et al.*, 2013). The dorsal stream in humans was considered predominantly involved in planning vocal muscle actions, in other words, principally for the speaking production (Hickok *et al.*, 2003). The dorsal stream provides the interface of auditory and motor cooperation process by performing phonological planning of sound-to-articulation representations, which is sub-served by projections from auditory cortical circuits to temporoparietal and frontal networks (Rauschecker and Scott, 2009; Friederici, 2012a; Friederici and Gierhan, 2013; Cahana-Amity and Albert, 2014). This cooperation process involves the motor mechanism was suggested to be related to the error of no response during stimulation (Fridriksson *et al.*, 2018). These studies showed that the dorsal stream plays an important role in processing auditory signals and phonological production. Under TMS stimulation, those naming errors were produced mainly due to the interruption of signal interaction on the dorsal stream for phonological motion control.

Regarding their difference, the ventral stream is mainly associated with auditory object recognition and commutative combinatorics. In contrast, the dorsal stream is related to the hierarchical predictive coding of sequences from phonemes to words and sentences (Bornkessel-Schlesewsky *et al.*, 2015). Motor speech impairments mostly involve damage to the dorsal stream, whereas measures of impaired speech comprehension are more strongly associated with the ventral stream (Fridriksson *et al.*, 2018). As a summary, it can be concluded that the difference between perceptual (echoic) and phonological-articulatory (motor) aspects of language functions emerge from the separate contribution of dorsal and ventral streams (Buchsbaum *et al.*, 2005).

In summary, the naming errors that occur under the stimulation of nTMS might not be the result of disrupting a single stream but might be due to the cooperation of the dorsal and ventral streams being disturbed simultaneously. So far, the understanding of dorsal and ventral stream-related tracts was only related to the level of anatomy and external functional performance. However, the investigation on different types of naming errors gives insight into processing and language generation on different levels. This suggests that the functional collaboration between dorsal and ventral streams may be hierarchical or multi-layered, which requires further investigations. Future studies using external interferences, such as nTMS, to interrupt the information processing of language and interaction with other cortical regions can enrich and improve the dual-stream hypothesis.

5.6 Adjustments of Parameters in DTI-FT

The accuracy of the FA value is affected by various factors, such as scanning parameters (the number of DTI gradients and voxel resolution), partial volume effects, signal-to-noise ratio, spatial resolution, scanner model, and diffusion encoding direction (Bourne *et al.*, 2017). In 2018, Kronlage's study found a negative correlation between FA and weight, height, and age in normal individuals and suggested that FA tends to be lower in men than women (Kronlage *et al.*, 2018). However, FA is used as a measurement for the integrity of cerebral microstructures due to its sensitivity in detecting micro-changes. The differences between FA in normal individuals have not been fully elucidated and understood and the range of FA in normal subjects still requires further inspection. So, one might argue that relying on FA for clinical purposes is premature.

Regarding its scientific application, FA is an important parameter in DTI related studies. Domin's study demonstrated that the thresholds of parameters combined with the highest FA showed the highest effects on the tractography results; meanwhile, limits on angulation and fiber length influenced its lateralization effects (Domin *et al.*, 2014). Taoka found that different FA thresholds would affect correlation levels between diffusion tensor parameters and the severity of Alzheimer's Disease. It was concluded that a high correlation could be observed under the FA threshold at 0.2 between mean apparent diffusion coefficient (ADC) values and Mini-Mental State Examination (MMSE) scores (Taoka *et al.*, 2009).

In most tractography analyses, the setup of the FT threshold is often based on a single fixed FA, such as FA = 0.1. This setting does not take the differences between individuals into account, nor the differences in the shape and volume of the skull that may affect the distribution

of the MRI magnetic field. These factors may interfere with the size of the individual's absolute FA value. Until now, there is no consensus on the adjustment of FA for DTI-FT. Regrading those issues, Niida carried out an evaluation on the integrity of the anterior thalamic radiation (ATR) to adjusting the FA value to the optimal level in a study on Bipolar Dis-ease (Niida *et al.*, 2018). The most frequently used method includes quartile individual FAT or fixed parameters like the FA value (Weiss *et al.*, 2015; Ille *et al.*, 2018; Sollmann *et al.*, 2018c). The quartile setup of FA in FT was used in previous studies to optimize the visualization of intracranial tracts by Sollmann *et al.* (Frey *et al.*, 2012; Sollmann *et al.*, 2016b; Sollmann *et al.*, 2018c).

In the current study, when considering nine different subcortical language-related pathways known from previous pieces of literature, we applied both settings simultaneously (25%FAT, 50%FAT, 75%FAT, 100%FAT, and FA=0.1, FA=0.15) for constructing tractography. We compared them and aimed to find the optimal adjustment for the highest fraction of neural tracts' visualization. According to our knowledge, this approach has not been used in previous studies. It may give researchers a better chance to detect underlying changes in subcortical structures.

5.7 Limitation

While interpreting the results of the current study, its limitations should be considered at the same time.

First, from a technical point of view, the current DTI-FT technology had its own limitation, especially the reconstruction of crossing tracts or tracts in voxels located within the vicinity of the tumor or edema, which vulnerably results in an uncertainty of the tracked fibers (Berman *et al.*, 2007; Duffau, 2014). This reason leading to this limitation was reported both by Pul *et al.* and Wakana *et al.*, stating that the tracking excludes regions with planar anisotropy because no main direction of diffusion can be determined (Wakana *et al.*, 2004; van Pul *et al.*, 2006). Particularly, in seed-based tracking, fibers might be missing owing to inconsistent ROI location. Currently, in the neurosurgery department, DTI combined with deterministic tracking algorithms is used for routine practice. It should be considered to develop more advanced diffusion-weighted sequences and tractography algorithms to regress out the interference signals from edema or bleeding in future studies. This may improve the reliability and accuracy of the results (Tuch *et al.*, 2002; Yeh and Tseng, 2011; Hori *et al.*, 2012; Kuhnt *et al.*, 2013a; Kuhnt *et al.*, 2013b; Li *et al.*, 2013).

Second, it is demonstrated in the previous articles that nTMS language mapping is well correlated with results of intraoperative DES, especially in terms of negative mapping, which has been proved to be with high sensitivity (maximal to 92%) (Picht *et al.*, 2013; Krieg *et al.*, 2014b). Picht *et al.* reported that preoperative nTMS language mapping showed an overall sensitivity of 90.2% and specificity of 23.8% (positive predictive value of 35.6% and negative predictive value of 83.9%) compared with DES (Picht *et al.*, 2013). The low ratio of positive predictive value requires further investigations. It might be due to not all errors stemming from the language-eloquent cortex but stemming from language-related brain regions, which suggested that not all language-positive nTMS spots must be connected to essential subcortical tracts.

Third, subcortical language-related pathways from nTMS-based DTI-FT have not been validated by intraoperative DES, except for one case report (Sollmann *et al.*, 2015a). The language function was suggested to be dynamic in structural organizations so that it is still difficult to determine the roles of a single fascicle and the whole network on different components of language function. In addition, in this study, we were unable to determine whether the level of patients' language prognosis is directly related to the whole brain network, nor could we determine its associations with some single subcortical language-related pathway. Notably, it has recently been detected by Negwer *et al.* in the investigation of the language prognosis of patients receiving preoperative nTMS-based DTI-FT, indicated that the language status improved during clinical follow-up even in some patients with language deficits (Negwer *et al.*, 2018).

In the future, we should collect more data to confirm results and aim to provide accurate and function-specific tractography; meanwhile, systematic and multicentered comparisons of nTMS-based DTI-FT and subcortical intraoperative DES should be the next step.

6. SUMMARY

6.1 English

This is one of the first studies aiming at preoperative nTMS-based function-specific tractography.

Currently, the primary treatment for intracranial tumors is still surgical resection. It can be told that the combination of the preoperative nTMS language mapping and nTMS-based DTI-FT provides information of individually organized language-related tracts for optimizing the tumor resection process, for example, selecting the proper surgical approach to lower the risk of injury to important tracts, decreasing the size of the surgical skull window, so that to protect the cerebral function. Regarding the results of fiber tracking, the category of all errors except hesitations is of practical significance to comprehensively indicate the individual language-related cortical and subcortical structures. This can reduce the complexity of clinical analysis and offer more convenient and effective references for clinical decisions.

The clinical outcomes of the patients in the current study demonstrated that this combination could benefit the functional prognosis in the long term. When the tumor location is within the traditionally defined function eloquent cerebral regions, nTMS is an effective method to assist in deciding whether the patient still has the opportunity to undergo resection.

By comparing different settings and employing different language error types as regions of interest, we can further analyze tractography results for the best visualization of language-related tracts, consisting of AF, SLF, ILF, UF, FoF, CF, CNT, CtF, and ArF. Analysis based on different types of naming errors provides more detailed information for understanding the organization of language in the brain. Different neural tracts in different categories of naming errors were visualized at different frequencies. Those findings of the current study were basically similar to those observed in previous studies. However, it cannot be simply interpreted that the most visualized tracts based on the seed of one category were the main factor leading to the corresponding naming error. Based on current findings, it can be concluded that language processing cannot be tributed to certain nerve bundles but to the hierarchical cooperation and information interaction among different cerebral fibers. Different neural tracts and cortical regions form language-related networks to maintain relevant brain functions.

This study also analyzed the subcortical fibers based on the dual-stream hypothesis, further explaining that the naming errors cannot be attributed to a single stream. The hierarchical or multi-layered collaboration between dorsal and ventral streams should be considered when analyzing their functional organization.

In summary, function-specific nTMS-based DTI-FT can potentially benefit intraoperative guidance and lead to a better prognosis during clinical follow-up. Further validation of the presented approach by intraoperative DES is needed. In the future, the analysis of language and even motor functions should be based on brain neural networks and the collaboration within and between networks to be more in line with the brain's biological structure.

6.2 Deutsch

Dies ist eine der ersten Studien zur präoperativen, nTMS-basierten und funktionsspezifischen Traktographie.

Derzeit ist die chirurgische Resektion immernoch die primäre Behandlung für intrakranielle Tumore. Es konnte festgestellt werden, dass die Kombination aus präoperativem nTMS-Sprachmapping und nTMS-basiertem DTI-FT Informationen zu den individuell organisierten, sprachbezogenen Faserbahnen liefert und durch die Optimierung des Tumorsektionsprozesses dazu beiträgt die Gehirnfunktion zu schützen, z. B. durch die Auswahl des geeigneten chirurgischen Ansatzes, durch die Verringerung des Verletzungsrisikos wichtiger Trakte sowie durch die Verkleinerung des operativen Zugangs. In Bezug auf die Ergebnisse der Faserdarstellung ist die Kategorie „Fehler exklusive des Zögerns“ von praktischer Bedeutung, um die einzelnen sprachbezogenen kortikalen und subkortikalen Strukturen umfassend darzustellen. Dies kann die Komplexität der klinischen Analyse verringern, indem es einfachere und effektivere Referenzen für klinische Entscheidungen bietet. Die klinischen Verläufe der Patienten in der Studie zeigten, dass diese Kombination das funktionelle Ergebnis langfristig verbessern kann. Wenn sich der Tumor innerhalb der traditionell als funktionseloquent definierten Gehirnregionen befindet, ist nTMS eine wirksame Methode, um zu entscheiden, ob für den Patient noch die Möglichkeit einer Resektion besteht.

Durch den Vergleich verschiedener Einstellungen des DTI-FT und die Verwendung verschiedener Sprachfehlertypen zur Definition relevanter Gehirnregionen, können die Traktographieergebnisse vertieft analysiert werden, um die bestmögliche Visualisierung der sprachbezogenen Trakte zu erhalten, welche aus AF, SLF, ILF, UF, FoF, CF, CNT, CtF und ArF bestehen. Die auf den verschiedenen Typen von Benennungsfehlern basierende Analyse liefert detailliertere Informationen zum Verständnis der Organisation der Sprache im Gehirn. Die verschiedenen neuronalen Bahnen konnten durch die verschiedenen Kategorien der Benennungsfehler unterschiedlich abgebildet werden. Diese Ergebnisse der aktuellen Studie decken sich im Wesentlichen mit Beobachtungen früherer Studien. Es kann jedoch nicht einfach geschlossen werden, dass die Faserbahnen, die am deutlichsten durch die Verwendung einer Fehlerkategorien als Startwerte dargestellt werden, auch hauptsächlich für den entsprechenden Benennungsfehler sind. Aus den aktuellen Ergebnissen kann geschlossen werden, dass die Sprachverarbeitung nicht bestimmten Nervenbündeln zugeordnet werden kann, sondern auf der hierarchischen Zusammenarbeit und dem Informationsaustausch verschiedener Hirnfasern beruht. Verschiedene Nervenbahnen und kortikale Regionen bilden sprachbezogene Netzwerke, um die relevanten Gehirnfunktionen aufrechtzuerhalten.

In der Studie wurden die subkortikalen Fasern auch basierend auf der Dual-Stream-Hypothese analysiert und es zeigte sich, dass die Namensfehler nicht einem einzelnen Strom zugeordnet

werden können. Die hierarchische oder mehrschichtige Zusammenarbeit zwischen den dorsalen und ventralen Strömen sollte bei der Analyse ihrer funktionellen Organisation berücksichtigt werden.

Zusammenfassend kann ein funktionsspezifisches nTMS-basiertes DTI-FT möglicherweise für die intraoperative Orientierung von Vorteil sein und zu einer verbesserten Prognose in der klinischen Nachsorge führen. Eine weitere Validierung der vorgestellten Methode durch intraoperatives DES ist erforderlich. In Zukunft sollte die Analyse der sprachlichen und auch motorischen Funktionen auf den neuronalen Netzen des Gehirns und der Zusammenarbeit innerhalb und zwischen diesen Netzwerken basieren, um der biologischen Struktur des Gehirns besser zu entsprechen.

7. REFERENCES

- Adamson DC, Rasheed BA, McLendon RE, Bigner DD. Central nervous system. *Cancer Biomark* 2010; 9(1-6): 193-210.
- Ahmadipour Y, Kaur M, Pierscianek D, Gembruch O, Oppong MD, Mueller O, *et al.* Association of Surgical Resection, Disability, and Survival in Patients with Glioblastoma. *J Neurol Surg A Cent Eur Neurosurg* 2019; 80(4): 262-8.
- Axer H, Klingner CM, Prescher A. Fiber anatomy of dorsal and ventral language streams. *Brain Lang* 2013; 127(2): 192-204.
- Barker AT, Jalinous R, Freeston IL. Non-invasive magnetic stimulation of human motor cortex. *Lancet* 1985; 1(8437): 1106-7.
- Basser PJ, Pierpaoli C. Microstructural and physiological features of tissues elucidated by quantitative-diffusion-tensor MRI. *J Magn Reson B* 1996; 111(3): 209-19.
- Berman JI, Berger MS, Chung SW, Nagarajan SS, Henry RG. Accuracy of diffusion tensor magnetic resonance imaging tractography assessed using intraoperative subcortical stimulation mapping and magnetic source imaging. *J Neurosurg* 2007; 107(3): 488-94.
- Bernal B, Ardila A. The role of the arcuate fasciculus in conduction aphasia. *Brain* 2009; 132(Pt 9): 2309-16.
- Bhatnagar SC. *Neuroscience for the study of communicative disorders*. Fifth edition. ed. Philadelphia: Wolters Kluwer; 2018.
- Borchers S, Himmelbach M, Logothetis N, Karnath HO. Direct electrical stimulation of human cortex - the gold standard for mapping brain functions? *Nat Rev Neurosci* 2011; 13(1): 63-70.
- Bornkessel-Schlesewsky I, Schlesewsky M, Small SL, Rauschecker JP. Neurobiological roots of language in primate audition: common computational properties. *Trends Cogn Sci* 2015; 19(3): 142-50.
- Bourne R, Liang S, Panagiotaki E, Bongers A, Sved P, Watson G. Measurement and modeling of diffusion time dependence of apparent diffusion coefficient and fractional anisotropy in prostate tissue *ex vivo*. *NMR Biomed* 2017; 30(10).
- Brasil-Neto JP, Cohen LG, Panizza M, Nilsson J, Roth BJ, Hallett M. Optimal focal transcranial magnetic activation of the human motor cortex: effects of coil orientation, shape of the induced current pulse, and stimulus intensity. *J Clin Neurophysiol* 1992; 9(1): 132-6.
- Brell M, Ibanez J, Caral L, Ferrer E. Factors influencing surgical complications of intra-axial brain tumours. *Acta Neurochir (Wien)* 2000; 142(7): 739-50.
- Bridgers SL. The safety of transcranial magnetic stimulation reconsidered: evidence regarding cognitive and other cerebral effects. *Electroencephalogr Clin Neurophysiol Suppl* 1991; 43: 170-9.
- Broce IJ, Bernal B, Altman N, Bradley C, Baez N, Cabrera L, *et al.* Fiber pathways supporting early literacy development in 5-8-year-old children. *Brain Cogn* 2019; 134: 80-9.
- Buchsbaum BR, Olsen RK, Koch P, Berman KF. Human dorsal and ventral auditory streams subserve rehearsal-based and echoic processes during verbal working memory. *Neuron* 2005; 48(4): 687-97.
- Burgel U, Madler B, Honey CR, Thron A, Gilsbach J, Coenen VA. Fiber tracking with distinct software tools results in a clear diversity in anatomical fiber tract portrayal. *Cent Eur Neurosurg* 2009; 70(1): 27-35.
- Cahana-Amitay D, Albert ML. Brain and language: evidence for neural multifunctionality. *Behav Neurol* 2014; 2014: 260381.
- Calautti C, Leroy F, Guincestre JY, Marie RM, Baron JC. Sequential activation brain mapping after subcortical stroke: changes in hemispheric balance and recovery. *Neuroreport* 2001; 12(18): 3883-6.
- Catani M, Thiebaut de Schotten M. A diffusion tensor imaging tractography atlas for virtual *in vivo* dissections. *Cortex* 2008; 44(8): 1105-32.
- Chang EF, Raygor KP, Berger MS. Contemporary model of language organization: an overview for neurosurgeons. *Journal of neurosurgery* 2015; 122(2): 250-61.

Chang SM, Parney IF, McDermott M, Barker FG, 2nd, Schmidt MH, Huang W, *et al.* Perioperative complications and neurological outcomes of first and second craniotomies among patients enrolled in the Glioma Outcome Project. *J Neurosurg* 2003; 98(6): 1175-81.

Conner AK, Briggs RG, Sali G, Rahimi M, Baker CM, Burks JD, *et al.* A Connectomic Atlas of the Human Cerebrum-Chapter 13: Tractographic Description of the Inferior Fronto-Occipital Fasciculus. *Oper Neurosurg (Hagerstown)* 2018; 15(suppl_1): S436-S43.

Corina DP, Loudermilk BC, Detwiler L, Martin RF, Brinkley JF, Ojemann G. Analysis of naming errors during cortical stimulation mapping: implications for models of language representation. *Brain Lang* 2010; 115(2): 101-12.

Crosson B. Thalamic mechanisms in language: a reconsideration based on recent findings and concepts. *Brain Lang* 2013; 126(1): 73-88.

de Heer WA, Huth AG, Griffiths TL, Gallant JL, Theunissen FE. The Hierarchical Cortical Organization of Human Speech Processing. *J Neurosci* 2017; 37(27): 6539-57.

Deng ZD, Lisanby SH, Peterchev AV. Electric field depth-focality tradeoff in transcranial magnetic stimulation: simulation comparison of 50 coil designs. *Brain Stimul* 2013; 6(1): 1-13.

Dittinger E, Valizadeh SA, Jancke L, Besson M, Elmer S. Increased functional connectivity in the ventral and dorsal streams during retrieval of novel words in professional musicians. *Hum Brain Mapp* 2018; 39(2): 722-34.

Domin M, Langner S, Hosten N, Lotze M. Comparison of parameter threshold combinations for diffusion tensor tractography in chronic stroke patients and healthy subjects. *PLoS One* 2014; 9(5): e98211.

Duffau H. Brain mapping from neural basis of cognition to surgical applications. Vienna ; New York: SpringerWienNewYork,; 2011. p. 1 online resource (xii, 392 p).

Duffau H. Diffusion tensor imaging is a research and educational tool, but not yet a clinical tool. *World Neurosurg* 2014; 82(1-2): e43-5.

Duffau H, Capelle L, Denvil D, Sichez N, Gatignol P, Lopes M, *et al.* Functional recovery after surgical resection of low grade gliomas in eloquent brain: hypothesis of brain compensation. *J Neurol Neurosurg Psychiatry* 2003; 74(7): 901-7.

Duffau H, Capelle L, Sichez N, Denvil D, Lopes M, Sichez JP, *et al.* Intraoperative mapping of the subcortical language pathways using direct stimulations. An anatomo-functional study. *Brain* 2002; 125(Pt 1): 199-214.

Duffau H, Gatignol P, Moritz-Gasser S, Mandonnet E. Is the left uncinate fasciculus essential for language? A cerebral stimulation study. *J Neurol* 2009a; 256(3): 382-9.

Duffau H, Mandonnet E. The "onco-functional balance" in surgery for diffuse low-grade glioma: integrating the extent of resection with quality of life. *Acta Neurochir (Wien)* 2013; 155(6): 951-7.

Duffau H, Moritz-Gasser S, Gatignol P. Functional outcome after language mapping for insular World Health Organization Grade II gliomas in the dominant hemisphere: experience with 24 patients. *Neurosurg Focus* 2009b; 27(2): E7.

Duffau H, Peggy Gatignol ST, Mandonnet E, Capelle L, Taillandier L. Intraoperative subcortical stimulation mapping of language pathways in a consecutive series of 115 patients with Grade II glioma in the left dominant hemisphere. *J Neurosurg* 2008; 109(3): 461-71.

Epstein CM, Meador KJ, Loring DW, Wright RJ, Weissman JD, Sheppard S, *et al.* Localization and characterization of speech arrest during transcranial magnetic stimulation. *Clin Neurophysiol* 1999; 110(6): 1073-9.

Ewert S, Plettig P, Li N, Chakravarty MM, Collins DL, Herrington TM, *et al.* Toward defining deep brain stimulation targets in MNI space: A subcortical atlas based on multimodal MRI, histology and structural connectivity. *Neuroimage* 2018; 170: 271-82.

Fekonja L, Wang Z, Bahrend I, Rosenstock T, Rosler J, Wallmeroth L, *et al.* Manual for clinical language tractography. *Acta Neurochir (Wien)* 2019; 161(6): 1125-37.

Fornito A, Harrison BJ, Zalesky A, Simons JS. Competitive and cooperative dynamics of large-scale brain functional networks supporting recollection. *Proc Natl Acad Sci U S A* 2012; 109(31): 12788-93.

Frey D, Strack V, Wiener E, Jussen D, Vajkoczy P, Picht T. A new approach for corticospinal tract reconstruction based on navigated transcranial stimulation and standardized fractional anisotropy values. *Neuroimage* 2012; 62(3): 1600-9.

Fridriksson J, den Ouden DB, Hillis AE, Hickok G, Rorden C, Basilakos A, *et al.* Anatomy of aphasia revisited. *Brain* 2018; 141(3): 848-62.

Fridriksson J, Yourganov G, Bonilha L, Basilakos A, Den Ouden DB, Rorden C. Revealing the dual streams of speech processing. *Proc Natl Acad Sci U S A* 2016; 113(52): 15108-13.

Friederici AD. The brain basis of language processing: from structure to function. *Physiol Rev* 2011; 91(4): 1357-92.

Friederici AD. The cortical language circuit: from auditory perception to sentence comprehension. *Trends Cogn Sci* 2012a; 16(5): 262-8.

Friederici AD. Language development and the ontogeny of the dorsal pathway. *Front Evol Neurosci* 2012b; 4: 3.

Friederici AD, Gierhan SM. The language network. *Curr Opin Neurobiol* 2013; 23(2): 250-4.

Frost SB, Barbay S, Friel KM, Plautz EJ, Nudo RJ. Reorganization of remote cortical regions after ischemic brain injury: a potential substrate for stroke recovery. *J Neurophysiol* 2003; 89(6): 3205-14.

Futai M. Reconstitution of ATPase activity from the isolated alpha, beta, and gamma subunits of the coupling factor, F₁, of *Escherichia coli*. *Biochem Biophys Res Commun* 1977; 79(4): 1231-7.

Galantucci S, Tartaglia MC, Wilson SM, Henry ML, Filippi M, Agosta F, *et al.* White matter damage in primary progressive aphasias: a diffusion tensor tractography study. *Brain* 2011; 134(Pt 10): 3011-29.

Gierhan SM. Connections for auditory language in the human brain. *Brain Lang* 2013; 127(2): 205-21.

Gordon EM, Laumann TO, Gilmore AW, Newbold DJ, Greene DJ, Berg JJ, *et al.* Precision Functional Mapping of Individual Human Brains. *Neuron* 2017; 95(4): 791-807 e7.

Green CR, Lebel C, Rasmussen C, Beaulieu C, Reynolds JN. Diffusion tensor imaging correlates of saccadic reaction time in children with fetal alcohol spectrum disorder. *Alcohol Clin Exp Res* 2013; 37(9): 1499-507.

Groppa S, Oliviero A, Eisen A, Quartarone A, Cohen LG, Mall V, *et al.* A practical guide to diagnostic transcranial magnetic stimulation: report of an IFCN committee. *Clin Neurophysiol* 2012; 123(5): 858-82.

Halpern H. Language and motor speech disorders in adults. Austin, Tex.: Pro-Ed, Inc.; 1986.

Hamalainen S, Sairanen V, Leminen A, Lehtonen M. Bilingualism modulates the white matter structure of language-related pathways. *Neuroimage* 2017; 152: 249-57.

Hauck T, Probst M, Zimmer C, Ringel F, Meyer B, Wohlschlaeger A, *et al.* Language function shows comparable cortical patterns by functional MRI and repetitive nTMS in healthy volunteers. *Brain Imaging Behav* 2018.

Henry ML, Wilson SM, Babiak MC, Mandelli ML, Beeson PM, Miller ZA, *et al.* Phonological Processing in Primary Progressive Aphasia. *J Cogn Neurosci* 2016; 28(2): 210-22.

Herbet G, Zemmoura I, Duffau H. Functional Anatomy of the Inferior Longitudinal Fasciculus: From Historical Reports to Current Hypotheses. *Front Neuroanat* 2018; 12: 77.

Hernandez-Pavon JC, Makela N, Lehtinen H, Lioumis P, Makela JP. Effects of navigated TMS on object and action naming. *Frontiers in human neuroscience* 2014; 8: 660.

Hickok G, Buchsbaum B, Humphries C, Muftuler T. Auditory-motor interaction revealed by fMRI: speech, music, and working memory in area Spt. *J Cogn Neurosci* 2003; 15(5): 673-82.

Hickok G, Poeppel D. Dorsal and ventral streams: a framework for understanding aspects of the functional anatomy of language. *Cognition* 2004; 92(1-2): 67-99.

Hickok G, Poeppel D. The cortical organization of speech processing. *Nat Rev Neurosci* 2007; 8(5): 393-402.

Hillis AE, Beh YY, Sebastian R, Breining B, Tippett DC, Wright A, *et al.* Predicting recovery in acute poststroke aphasia. *Ann Neurol* 2018; 83(3): 612-22.

Hori M, Fukunaga I, Masutani Y, Taoka T, Kamagata K, Suzuki Y, *et al.* Visualizing non-Gaussian diffusion: clinical application of q-space imaging and diffusional kurtosis imaging of the brain and spine. *Magn Reson Med Sci* 2012; 11(4): 221-33.

Huber W, Poeck K, Willmes K. The Aachen Aphasia Test. *Adv Neurol* 1984; 42: 291-303.

Ille S, Engel L, Kelm A, Meyer B, Krieg SM. Language-Eloquent White Matter Pathway Tractography and the Course of Language Function in Glioma Patients. *Front Oncol* 2018; 8: 572.

Ille S, Sollmann N, Hauck T, Maurer S, Tanigawa N, Obermueller T, *et al.* Impairment of preoperative language mapping by lesion location: a functional magnetic resonance imaging, navigated transcranial magnetic stimulation, and direct cortical stimulation study. *J Neurosurg* 2015; 123(2): 314-24.

Indefrey P, Levelt WJ. The spatial and temporal signatures of word production components. *Cognition* 2004; 92(1-2): 101-44.

Jack CR, Jr., Thompson RM, Butts RK, Sharbrough FW, Kelly PJ, Hanson DP, *et al.* Sensory motor cortex: correlation of presurgical mapping with functional MR imaging and invasive cortical mapping. *Radiology* 1994; 190(1): 85-92.

Julkunen P, Kononen M, Maatta S, Tarkka IM, Hiekkala SH, Saisanen L, *et al.* Longitudinal study on modulated corticospinal excitability throughout recovery in supratentorial stroke. *Neurosci Lett* 2016; 617: 88-93.

Kamali A, Flanders AE, Brody J, Hunter JV, Hasan KM. Tracing superior longitudinal fasciculus connectivity in the human brain using high resolution diffusion tensor tractography. *Brain Struct Funct* 2014; 219(1): 269-81.

Kekhia H, Rigolo L, Norton I, Golby AJ. Special surgical considerations for functional brain mapping. *Neurosurg Clin N Am* 2011; 22(2): 111-32, vii.

Kelm A, Sollmann N, Ille S, Meyer B, Ringel F, Krieg SM. Resection of Gliomas with and without Neuropsychological Support during Awake Craniotomy-Effects on Surgery and Clinical Outcome. *Front Oncol* 2017; 7: 176.

Klostermann F, Krugel LK, Ehlen F. Functional roles of the thalamus for language capacities. *Front Syst Neurosci* 2013; 7: 32.

Koponen LM, Nieminen JO, Ilmoniemi RJ. Minimum-energy coils for transcranial magnetic stimulation: application to focal stimulation. *Brain Stimul* 2015; 8(1): 124-34.

Koponen LM, Nieminen JO, Ilmoniemi RJ. Multi-locus transcranial magnetic stimulation-theory and implementation. *Brain Stimul* 2018; 11(4): 849-55.

Krieg SM. Navigated transcranial magnetic stimulation in neurosurgery. Cham: Springer,; 2017. p. 1 online resource.

Krieg SM, Buchmann NH, Gempt J, Shiban E, Meyer B, Ringel F. Diffusion tensor imaging fiber tracking using navigated brain stimulation--a feasibility study. *Acta Neurochir (Wien)* 2012a; 154(3): 555-63.

Krieg SM, Lioumis P, Makela JP, Wilenius J, Karhu J, Hannula H, *et al.* Protocol for motor and language mapping by navigated TMS in patients and healthy volunteers; workshop report. *Acta Neurochir (Wien)* 2017; 159(7): 1187-95.

Krieg SM, Sabih J, Bulubasova L, Obermueller T, Negwer C, Janssen I, *et al.* Preoperative motor mapping by navigated transcranial magnetic brain stimulation improves outcome for motor eloquent lesions. *Neuro Oncol* 2014a; 16(9): 1274-82.

Krieg SM, Shiban E, Buchmann N, Gempt J, Foerschler A, Meyer B, *et al.* Utility of presurgical navigated transcranial magnetic brain stimulation for the resection of tumors in eloquent motor areas. *J Neurosurg* 2012b; 116(5): 994-1001.

Krieg SM, Shiban E, Buchmann N, Meyer B, Ringel F. Presurgical navigated transcranial magnetic brain stimulation for recurrent gliomas in motor eloquent areas. *Clin Neurophysiol* 2013; 124(3): 522-7.

Krieg SM, Sollmann N, Obermueller T, Sabih J, Bulubas L, Negwer C, *et al.* Changing the clinical course of glioma patients by preoperative motor mapping with navigated transcranial magnetic brain stimulation. *BMC Cancer* 2015; 15: 231.

Krieg SM, Sollmann N, Tanigawa N, Foerschler A, Meyer B, Ringel F. Cortical distribution of speech and language errors investigated by visual object naming and navigated transcranial magnetic stimulation. *Brain Struct Funct* 2016; 221(4): 2259-86.

Krieg SM, Tarapore PE, Picht T, Tanigawa N, Houde J, Sollmann N, *et al.* Optimal timing of pulse onset for language mapping with navigated repetitive transcranial magnetic stimulation. *NeuroImage* 2014b; 100: 219-36.

Kronlage M, Schwehr V, Schwarz D, Godel T, Uhlmann L, Heiland S, *et al.* Peripheral nerve diffusion tensor imaging (DTI): normal values and demographic determinants in a cohort of 60 healthy individuals. *Eur Radiol* 2018; 28(5): 1801-8.

Kuhnt D, Bauer MH, Becker A, Merhof D, Zolal A, Richter M, *et al.* Intraoperative visualization of fiber tracking based reconstruction of language pathways in glioma surgery. *Neurosurgery* 2012; 70(4): 911-9; discussion 9-20.

Kuhnt D, Bauer MH, Egger J, Richter M, Kapur T, Sommer J, *et al.* Fiber tractography based on diffusion tensor imaging compared with high-angular-resolution diffusion imaging with compressed sensing: initial experience. *Neurosurgery* 2013a; 72 Suppl 1: 165-75.

Kuhnt D, Bauer MH, Sommer J, Merhof D, Nimsky C. Optic radiation fiber tractography in glioma patients based on high angular resolution diffusion imaging with compressed sensing compared with diffusion tensor imaging - initial experience. *PLoS One* 2013b; 8(7): e70973.

Kummerer D, Hartwigsen G, Kellmeyer P, Glauche V, Mader I, Kloppel S, *et al.* Damage to ventral and dorsal language pathways in acute aphasia. *Brain* 2013; 136(Pt 2): 619-29.

Lebel C, Shaywitz B, Holahan J, Shaywitz S, Marchione K, Beaulieu C. Diffusion tensor imaging correlates of reading ability in dysfluent and non-impaired readers. *Brain Lang* 2013; 125(2): 215-22.

Leclercq D, Duffau H, Delmaire C, Capelle L, Gatignol P, Ducros M, *et al.* Comparison of diffusion tensor imaging tractography of language tracts and intraoperative subcortical stimulations. *J Neurosurg* 2010; 112(3): 503-11.

Lehericy S, Duffau H, Cornu P, Capelle L, Pidoux B, Carpentier A, *et al.* Correspondence between functional magnetic resonance imaging somatotopy and individual brain anatomy of the central region: comparison with intraoperative stimulation in patients with brain tumors. *J Neurosurg* 2000; 92(4): 589-98.

Lehtinen H, Makela JP, Makela T, Lioumis P, Metsahonkala L, Hokkanen L, *et al.* Language mapping with navigated transcranial magnetic stimulation in pediatric and adult patients undergoing epilepsy surgery: Comparison with extraoperative direct cortical stimulation. *Epilepsia Open* 2018; 3(2): 224-35.

Li X, Black M, Xia S, Zhan C, Bertisch HC, Branch CA, *et al.* Subcortical structure alterations impact language processing in individuals with schizophrenia and those at high genetic risk. *Schizophr Res* 2015; 169(1-3): 76-82.

Li Z, Peck KK, Brennan NP, Jenabi M, Hsu M, Zhang Z, *et al.* Diffusion tensor tractography of the arcuate fasciculus in patients with brain tumors: Comparison between deterministic and probabilistic models. *J Biomed Sci Eng* 2013; 6(2): 192-200.

Liang J, Lv X, Lu C, Ye X, Chen X, Fu J, *et al.* Prognostic factors of patients with Gliomas - an analysis on 335 patients with Glioblastoma and other forms of Gliomas. *BMC Cancer* 2020; 20(1): 35.

Liegeois FJ, Turner SJ, Mayes A, Bonthron AF, Boys A, Smith L, *et al.* Dorsal language stream anomalies in an inherited speech disorder. *Brain* 2019; 142(4): 966-77.

Lioumis P, Mustanoja S, Bikmullina R, Vitikainen AM, Kicic D, Salonen O, *et al.* Probing modifications of cortical excitability during stroke recovery with navigated transcranial magnetic stimulation. *Top Stroke Rehabil* 2012a; 19(2): 182-92.

Lioumis P, Zhdanov A, Makela N, Lehtinen H, Wilenius J, Neuvonen T, *et al.* A novel approach for documenting naming errors induced by navigated transcranial magnetic stimulation. *Journal of neuroscience methods* 2012b; 204(2): 349-54.

Loui P. A Dual-Stream Neuroanatomy of Singing. *Music Percept* 2015; 32(3): 232-41.

Love RJ, Webb WG. *Neurology for the speech-language pathologist*. 5th ed. St. Louis, MO: Mosby/Elsevier; 2008.

Lubrano V, Draper L, Roux FE. What makes surgical tumor resection feasible in Broca's area? Insights into intraoperative brain mapping. *Neurosurgery* 2010; 66(5): 868-75; discussion 75.

Maldonado IL, Moritz-Gasser S, de Champfleury NM, Bertram L, Moulinie G, Duffau H. Surgery for gliomas involving the left inferior parietal lobule: new insights into the functional anatomy provided by stimulation mapping in awake patients. *Journal of neurosurgery* 2011; 115(4): 770-9.

Mandonnet E, Nouet A, Gatignol P, Capelle L, Duffau H. Does the left inferior longitudinal fasciculus play a role in language? A brain stimulation study. *Brain* 2007; 130(Pt 3): 623-9.

Markwort S, Cordes P, Aldenhoff J. [Transcranial magnetic stimulation as an alternative to electroshock therapy in treatment resistant depressions. A literature review]. *Fortschr Neurol Psychiatr* 1997; 65(12): 540-9.

Matsuda M, Kohzuki H, Ishikawa E, Yamamoto T, Akutsu H, Takano S, *et al.* Prognostic analysis of patients who underwent gross total resection of newly diagnosed glioblastoma. *J Clin Neurosci* 2018; 50: 172-6.

Mayer L. Outcome after language mapping for glioma resection. *N Engl J Med* 2008; 358(16): 1750; author reply 1.

McCarron A, Chavez A, Babiak M, Berger MS, Chang EF, Wilson SM. Connected speech in transient aphasia after left hemisphere resective surgery. *Aphasiology* 2017; 31(11): 1266-81.

McKinnon ET, Fridriksson J, Basilakos A, Hickok G, Hillis AE, Spampinato MV, *et al.* Types of naming errors in chronic post-stroke aphasia are dissociated by dual stream axonal loss. *Sci Rep* 2018; 8(1): 14352.

Metoki A, Alm KH, Wang Y, Ngo CT, Olson IR. Never forget a name: white matter connectivity predicts person memory. *Brain Struct Funct* 2017; 222(9): 4187-201.

Meyer BU, Werhahn K, Rothwell JC, Roericht S, Fauth C. Functional organisation of corticonuclear pathways to motoneurons of lower facial muscles in man. *Exp Brain Res* 1994; 101(3): 465-72.

Morrison MA, Tam F, Garavaglia MM, Hare GM, Cusimano MD, Schweizer TA, *et al.* Sources of Variation Influencing Concordance between Functional MRI and Direct Cortical Stimulation in Brain Tumor Surgery. *Front Neurosci* 2016; 10: 461.

Muller L, Rolston JD, Fox NP, Knowlton R, Rao VR, Chang EF. Direct electrical stimulation of human cortex evokes high gamma activity that predicts conscious somatosensory perception. *J Neural Eng* 2018; 15(2): 026015.

Mulroy E, Murphy S, Lynch T. Alexia without agraphia. *Ir Med J* 2011; 104(4): 124.

Nahas Z, Molloy MA, Hughes PL, Oliver NC, Arana GW, Risch SC, *et al.* Repetitive transcranial magnetic stimulation: perspectives for application in the treatment of bipolar and unipolar disorders. *Bipolar Disord* 1999; 1(2): 73-80.

Najib U, Bashir S, Edwards D, Rotenberg A, Pascual-Leone A. Transcranial brain stimulation: clinical applications and future directions. *Neurosurg Clin N Am* 2011; 22(2): 233-51, ix.

Nakajima R, Kinoshita M, Shinohara H, Nakada M. The superior longitudinal fascicle: reconsidering the fronto-parietal neural network based on anatomy and function. *Brain Imaging Behav* 2019.

Negwer C, Beurskens E, Sollmann N, Maurer S, Ille S, Giglhuber K, *et al.* Loss of Subcortical Language Pathways Correlates with Surgery-Related Aphasia in Patients with Brain Tumor: An Investigation via Repetitive Navigated Transcranial Magnetic Stimulation-Based Diffusion Tensor Imaging Fiber Tracking. *World Neurosurg* 2018; 111: e806-e18.

Negwer C, Ille S, Hauck T, Sollmann N, Maurer S, Kirschke JS, *et al.* Visualization of subcortical language pathways by diffusion tensor imaging fiber tracking based on rTMS language mapping. *Brain Imaging Behav* 2017a; 11(3): 899-914.

Negwer C, Sollmann N, Ille S, Hauck T, Maurer S, Kirschke JS, *et al.* Language pathway tracking: comparing nTMS-based DTI fiber tracking with a cubic ROIs-based protocol. *J Neurosurg* 2017b; 126(3): 1006-14.

Niida R, Yamagata B, Niida A, Uechi A, Matsuda H, Mimura M. Aberrant Anterior Thalamic Radiation Structure in Bipolar Disorder: A Diffusion Tensor Tractography Study. *Front Psychiatry* 2018; 9: 522.

Niu C, Liu X, Yang Y, Zhang K, Min Z, Wang M, *et al.* Assessing Region of Interest Schemes for the Corticospinal Tract in Patients With Brain Tumors. *Medicine (Baltimore)* 2016; 95(12): e3189.

Northam GB, Morgan AT, Fitzsimmons S, Baldeweg T, Liegeois FJ. Corticobulbar Tract Injury, Oromotor Impairment and Language Plasticity in Adolescents Born Preterm. *Front Hum Neurosci* 2019; 13: 45.

Nosseck E, Matot I, Shahar T, Barzilai O, Rapoport Y, Gonen T, *et al.* Intraoperative seizures during awake craniotomy: incidence and consequences: analysis of 477 patients. *Neurosurgery* 2013a; 73(1): 135-40; discussion 40.

Nosseck E, Matot I, Shahar T, Barzilai O, Rapoport Y, Gonen T, *et al.* Failed awake craniotomy: a retrospective analysis in 424 patients undergoing craniotomy for brain tumor. *J Neurosurg* 2013b; 118(2): 243-9.

Ogunlade J, Wiginton JGt, Elia C, Odell T, Rao SC. Primary Spinal Astrocytomas: A Literature Review. *Cureus* 2019; 11(7): e5247.

Oliveira FF, Marin SM, Bertolucci PH. Neurological impressions on the organization of language networks in the human brain. *Brain Inj* 2017; 31(2): 140-50.

Ottenhausen M, Krieg SM, Meyer B, Ringel F. Functional preoperative and intraoperative mapping and monitoring: increasing safety and efficacy in glioma surgery. *Neurosurg Focus* 2015; 38(1): E3.

Paiva WS, Fonoff ET, Marcolin MA, Cabrera HN, Teixeira MJ. Cortical mapping with navigated transcranial magnetic stimulation in low-grade glioma surgery. *Neuropsychiatr Dis Treat* 2012; 8: 197-201.

Papagno C. Naming and the role of the uncinate fasciculus in language function. *Curr Neurol Neurosci Rep* 2011; 11(6): 553-9.

Papagno C, Miracapillo C, Casarotti A, Romero Lauro LJ, Castellano A, Falini A, *et al.* What is the role of the uncinate fasciculus? Surgical removal and proper name retrieval. *Brain* 2011; 134(Pt 2): 405-14.

Pascual-Leone A, Bartres-Faz D, Keenan JP. Transcranial magnetic stimulation: studying the brain-behaviour relationship by induction of 'virtual lesions'. *Philos Trans R Soc Lond B Biol Sci* 1999; 354(1387): 1229-38.

Pascual-Leone A, Gates JR, Dhuna A. Induction of speech arrest and counting errors with rapid-rate transcranial magnetic stimulation. *Neurology* 1991; 41(5): 697-702.

Peng Z, Zhou C, Xue S, Bai J, Yu S, Li X, *et al.* Mechanism of Repetitive Transcranial Magnetic Stimulation for Depression. *Shanghai Arch Psychiatry* 2018; 30(2): 84-92.

Peraud A, Ilmberger J, Reulen HJ. Surgical resection of gliomas WHO grade II and III located in the opercular region. *Acta Neurochir (Wien)* 2004; 146(1): 9-17; discussion -8.

Peus D, Newcomb N, Hofer S. Appraisal of the Karnofsky Performance Status and proposal of a simple algorithmic system for its evaluation. *BMC Med Inform Decis Mak* 2013; 13: 72.

Picht T, Krieg SM, Sollmann N, Rosler J, Niraula B, Neuvonen T, *et al.* A comparison of language mapping by preoperative navigated transcranial magnetic stimulation and direct cortical stimulation during awake surgery. *Neurosurgery* 2013; 72(5): 808-19.

Porter KR, McCarthy BJ, Berbaum ML, Davis FG. Conditional survival of all primary brain tumor patients by age, behavior, and histology. *Neuroepidemiology* 2011; 36(4): 230-9.

Quinones-Hinojosa A, Kaprelian T, Chaichana KL, Sanai N, Parsa AT, Berger MS, *et al.* Pre-operative factors affecting resectability of giant intracranial meningiomas. *Can J Neurol Sci* 2009; 36(5): 623-30.

Raffa G, Barend I, Schneider H, Faust K, Germano A, Vajkoczy P, *et al.* A Novel Technique for Region and Linguistic Specific nTMS-based DTI Fiber Tracking of Language Pathways in Brain Tumor Patients. *Front Neurosci* 2016; 10: 552.

Raffa G, Conti A, Scibilia A, Sindorio C, Quattropiani MC, Visocchi M, *et al.* Functional Reconstruction of Motor and Language Pathways Based on Navigated Transcranial Magnetic Stimulation and DTI Fiber Tracking for the Preoperative Planning of Low Grade Glioma Surgery: A New Tool for Preservation and Restoration of Eloquent Networks. *Acta Neurochir Suppl* 2017; 124: 251-61.

Rauschecker JP. Ventral and dorsal streams in the evolution of speech and language. *Front Evol Neurosci* 2012; 4: 7.

Rauschecker JP, Scott SK. Maps and streams in the auditory cortex: nonhuman primates illuminate human speech processing. *Nat Neurosci* 2009; 12(6): 718-24.

Ravazzani P, Ruohonen J, Grandori F, Tognola G. Magnetic stimulation of the nervous system: induced electric field in unbounded, semi-infinite, spherical, and cylindrical media. *Ann Biomed Eng* 1996; 24(5): 606-16.

Rees JH. Diagnosis and treatment in neuro-oncology: an oncological perspective. *Br J Radiol* 2011; 84 Spec No 2: S82-9.

Ripolles P, Rojo N, Grau-Sanchez J, Amengual JL, Camara E, Marco-Pallares J, *et al.* Music supported therapy promotes motor plasticity in individuals with chronic stroke. *Brain Imaging Behav* 2016; 10(4): 1289-307.

Riva M, Fava E, Gallucci M, Comi A, Casarotti A, Alfiero T, *et al.* Monopolar high-frequency language mapping: can it help in the surgical management of gliomas? A comparative clinical study. *J Neurosurg* 2016; 124(5): 1479-89.

Rolheiser T, Stamatakis EA, Tyler LK. Dynamic processing in the human language system: synergy between the arcuate fascicle and extreme capsule. *J Neurosci* 2011; 31(47): 16949-57.

Rossi A, Cetrano G, Pertile R, Rabbi L, Donisi V, Grigoletti L, *et al.* Burnout, compassion fatigue, and compassion satisfaction among staff in community-based mental health services. *Psychiatry Res* 2012; 200(2-3): 933-8.

Rossi E, Cheng H, Kroll JF, Diaz MT, Newman SD. Changes in White-Matter Connectivity in Late Second Language Learners: Evidence from Diffusion Tensor Imaging. *Front Psychol* 2017; 8: 2040.

Roth Y, Amir A, Levkovitz Y, Zangen A. Three-dimensional distribution of the electric field induced in the brain by transcranial magnetic stimulation using figure-8 and deep H-coils. *J Clin Neurophysiol* 2007; 24(1): 31-8.

Roth Y, Pell GS, Zangen A. Commentary on: Deng *et al.*, Electric field depth-focality tradeoff in transcranial magnetic stimulation: simulation comparison of 50 coil designs. *Brain Stimul* 2013; 6(1): 14-5.

Saito T, Muragaki Y, Miura I, Tamura M, Maruyama T, Nitta M, *et al.* Functional plasticity of language confirmed with intraoperative electrical stimulations and updated neuronavigation: case report of low-grade glioma of the left inferior frontal gyrus. *Neurol Med Chir (Tokyo)* 2014; 54(7): 587-92.

Sanai N, Mirzadeh Z, Berger MS. Functional outcome after language mapping for glioma resection. *N Engl J Med* 2008; 358(1): 18-27.

Saur D, Kreher BW, Schnell S, Kummerer D, Kellmeyer P, Vry MS, *et al.* Ventral and dorsal pathways for language. *Proc Natl Acad Sci U S A* 2008; 105(46): 18035-40.

Sawaya R, Hammoud M, Schoppa D, Hess KR, Wu SZ, Shi WM, *et al.* Neurosurgical outcomes in a modern series of 400 craniotomies for treatment of parenchymal tumors. *Neurosurgery* 1998; 42(5): 1044-55; discussion 55-6.

Schreckenberger M, Spetzger U, Sabri O, Meyer PT, Zeggel T, Zimny M, *et al.* Localisation of motor areas in brain tumour patients: a comparison of preoperative [¹⁸F]FDG-PET and intraoperative cortical electrostimulation. *Eur J Nucl Med* 2001; 28(9): 1394-403.

Schulz C, Waldeck S, Mauer UM. Intraoperative image guidance in neurosurgery: development, current indications, and future trends. *Radiol Res Pract* 2012; 2012: 197364.

Sharma N, Classen J, Cohen LG. Neural plasticity and its contribution to functional recovery. *Handb Clin Neurol* 2013; 110: 3-12.

Skorpil M, Rolheiser T, Robertson H, Sundin A, Svenningsson P. Diffusion tensor fiber tractography of the olfactory tract. *Magn Reson Imaging* 2011; 29(2): 289-92.

Sliwiska MW, Vitello S, Devlin JT. Transcranial magnetic stimulation for investigating causal brain-behavioral relationships and their time course. *J Vis Exp* 2014(89).

Sollmann N, Bulubas L, Tanigawa N, Zimmer C, Meyer B, Krieg SM. The variability of motor evoked potential latencies in neurosurgical motor mapping by preoperative navigated transcranial magnetic stimulation. *BMC Neurosci* 2017; 18(1): 5.

Sollmann N, Fuss-Ruppenthal S, Zimmer C, Meyer B, Krieg SM. Investigating Stimulation Protocols for Language Mapping by Repetitive Navigated Transcranial Magnetic Stimulation. *Front Behav Neurosci* 2018a; 12: 197.

Sollmann N, Giglhuber K, Tussis L, Meyer B, Ringel F, Krieg SM. nTMS-based DTI fiber tracking for language pathways correlates with language function and aphasia - A case report. *Clin Neurol Neurosurg* 2015a; 136: 25-8.

Sollmann N, Goblirsch-Kolb MF, Ille S, Butenschoen VM, Boeckh-Behrens T, Meyer B, *et al.* Comparison between electric-field-navigated and line-navigated TMS for cortical motor mapping in patients with brain tumors. *Acta Neurochir (Wien)* 2016a; 158(12): 2277-89.

Sollmann N, Hauck T, Hapfelmeier A, Meyer B, Ringel F, Krieg SM. Intra- and interobserver variability of language mapping by navigated transcranial magnetic brain stimulation. *BMC Neurosci* 2013; 14: 150.

Sollmann N, Ille S, Hauck T, Maurer S, Negwer C, Zimmer C, *et al.* The impact of preoperative language mapping by repetitive navigated transcranial magnetic stimulation on the clinical course of brain tumor patients. *BMC Cancer* 2015b; 15: 261.

Sollmann N, Ille S, Obermueller T, Negwer C, Ringel F, Meyer B, *et al.* The impact of repetitive navigated transcranial magnetic stimulation coil positioning and stimulation parameters on human language function. *Eur J Med Res* 2015c; 20: 47.

Sollmann N, Kelm A, Ille S, Schroder A, Zimmer C, Ringel F, *et al.* Setup presentation and clinical outcome analysis of treating highly language-eloquent gliomas via preoperative navigated transcranial magnetic stimulation and tractography. *Neurosurg Focus* 2018b; 44(6): E2.

Sollmann N, Negwer C, Ille S, Maurer S, Hauck T, Kirschke JS, *et al.* Feasibility of nTMS-based DTI fiber tracking of language pathways in neurosurgical patients using a fractional anisotropy threshold. *J Neurosci Methods* 2016b; 267: 45-54.

Sollmann N, Tanigawa N, Tussis L, Hauck T, Ille S, Maurer S, *et al.* Cortical regions involved in semantic processing investigated by repetitive navigated transcranial magnetic stimulation and object naming. *Neuropsychologia* 2015d; 70: 185-95.

Sollmann N, Wildschuetz N, Kelm A, Conway N, Moser T, Bulubas L, *et al.* Associations between clinical outcome and navigated transcranial magnetic stimulation characteristics in patients with motor-eloquent brain lesions: a combined navigated transcranial magnetic stimulation-diffusion tensor imaging fiber tracking approach. *J Neurosurg* 2018c; 128(3): 800-10.

Southwell DG, Hervey-Jumper SL, Perry DW, Berger MS. Intraoperative mapping during repeat awake craniotomy reveals the functional plasticity of adult cortex. *Journal of neurosurgery* 2016; 124(5): 1460-9.

Steinbrink C, Vogt K, Kastrup A, Muller HP, Juengling FD, Kassubek J, *et al.* The contribution of white and gray matter differences to developmental dyslexia: insights from DTI and VBM at 3.0 T. *Neuropsychologia* 2008; 46(13): 3170-8.

Strijkers K, Costa A. Riding the lexical speedway: a critical review on the time course of lexical selection in speech production. *Front Psychol* 2011; 2: 356.

Suri JS, Setarehdan SK, Singh S. *Advanced algorithmic approaches to medical image segmentation : state-of-the-art applications in cardiology, neurology, mammography and pathology.* London ; New York: Springer; 2002.

Tai YF, Piccini P. Applications of positron emission tomography (PET) in neurology. *J Neurol Neurosurg Psychiatry* 2004; 75(5): 669-76.

Talacchi A, Santini B, Casartelli M, Monti A, Capasso R, Miceli G. Awake surgery between art and science. Part II: language and cognitive mapping. *Funct Neurol* 2013; 28(3): 223-39.

Taoka T, Morikawa M, Akashi T, Miyasaka T, Nakagawa H, Kiuchi K, *et al.* Fractional anisotropy--threshold dependence in tract-based diffusion tensor analysis: evaluation of the uncinate fasciculus in Alzheimer disease. *AJNR Am J Neuroradiol* 2009; 30(9): 1700-3.

Tarapore PE, Findlay AM, Honma SM, Mizuiri D, Houde JF, Berger MS, *et al.* Language mapping with navigated repetitive TMS: proof of technique and validation. *Neuroimage* 2013; 82: 260-72.

Tate MC, Herbet G, Moritz-Gasser S, Tate JE, Duffau H. Probabilistic map of critical functional regions of the human cerebral cortex: Broca's area revisited. *Brain* 2014; 137(Pt 10): 2773-82.

Taylor MD, Bernstein M. Awake craniotomy with brain mapping as the routine surgical approach to treating patients with supratentorial intraaxial tumors: a prospective trial of 200 cases. *J Neurosurg* 1999; 90(1): 35-41.

Terao Y, Ugawa Y. Basic mechanisms of TMS. *J Clin Neurophysiol* 2002; 19(4): 322-43.

Tewarie P, Hillebrand A, van Dellen E, Schoonheim MM, Barkhof F, Polman CH, *et al.* Structural degree predicts functional network connectivity: a multimodal resting-state fMRI and MEG study. *Neuroimage* 2014; 97: 296-307.

Thielscher A, Kammer T. Linking physics with physiology in TMS: a sphere field model to determine the cortical stimulation site in TMS. *Neuroimage* 2002; 17(3): 1117-30.

Tomczak RJ, Wunderlich AP, Wang Y, Braun V, Antoniadis G, Gorich J, *et al.* fMRI for preoperative neurosurgical mapping of motor cortex and language in a clinical setting. *J Comput Assist Tomogr* 2000; 24(6): 927-34.

Toschi N, Welt T, Guerri M, Keck ME. A reconstruction of the conductive phenomena elicited by transcranial magnetic stimulation in heterogeneous brain tissue. *Phys Med* 2008; 24(2): 80-6.

Tuch DS, Reese TG, Wiegell MR, Makris N, Belliveau JW, Wedeen VJ. High angular resolution diffusion imaging reveals intravoxel white matter fiber heterogeneity. *Magn Reson Med* 2002; 48(4): 577-82.

van Pul C, Buijs J, Vilanova A, Roos FG, Wijn PF. Infants with perinatal hypoxic ischemia: feasibility of fiber tracking at birth and 3 months. *Radiology* 2006; 240(1): 203-14.

Wacker A, Holder M, Will BE, Winkler PA, Ilmberger J. [Comparison of the Aachen Aphasia Test, clinical study and Aachen Aphasia Beside Test in brain tumor patients]. *Nervenarzt* 2002; 73(8): 765-9.

Wakana S, Jiang H, Nagae-Poetscher LM, van Zijl PC, Mori S. Fiber tract-based atlas of human white matter anatomy. *Radiology* 2004; 230(1): 77-87.

Wang J, Meng HJ, Ji GJ, Jing Y, Wang HX, Deng XP, *et al.* Finger Tapping Task Activation vs. TMS Hotspot: Different Locations and Networks. *Brain Topogr* 2020; 33(1): 123-34.

Weiss C, Tursunova I, Neuschmelting V, Lockau H, Nettekoven C, Oros-Peusquens AM, *et al.* Improved nTMS- and DTI-derived CST tractography through anatomical ROI seeding on anterior pontine level compared to internal capsule. *Neuroimage Clin* 2015; 7: 424-37.

Wilson SM, Lam D, Babiak MC, Perry DW, Shih T, Hess CP, *et al.* Transient aphasias after left hemisphere resective surgery. *J Neurosurg* 2015; 123(3): 581-93.

Witruk E, Friederici AD, Lachmann T. Basic functions of language, reading and reading disability. Boston: Kluwer Academic Publishers; 2002.

Xu J, Elazab A, Liang J, Jia F, Zheng H, Wang W, *et al.* Cortical and Subcortical Structural Plasticity Associated with the Glioma Volumes in Patients with Cerebral Gliomas Revealed by Surface-Based Morphometry. *Front Neurol* 2017; 8: 266.

Yeh FC, Tseng WY. NTU-90: a high angular resolution brain atlas constructed by q-space diffeomorphic reconstruction. *Neuroimage* 2011; 58(1): 91-9.

Young RM, Jamshidi A, Davis G, Sherman JH. Current trends in the surgical management and treatment of adult glioblastoma. *Ann Transl Med* 2015; 3(9): 121.